INVITED PAPER

Co-Optimization of Power and Reserves in Dynamic T&D Power Markets With Nondispatchable Renewable Generation and Distributed Energy Resources

This paper presents a distributed, massively parallel architecture that enables tractable transmission and distribution locational marginal price (T&DLMP) discovery along with optimal scheduling of centralized generation, decentralized conventional and flexible loads, and distributed energy resources (DERs).

By Michael Caramanis, *Senior Member IEEE*, Elli Ntakou, *Student Member IEEE*, William W. Hogan, Aranya Chakrabortty, *Senior Member IEEE*, and Jens Schoene, *Member IEEE*

ABSTRACT | Marginal-cost-based dynamic pricing of electricity services, including real power, reactive power, and reserves, may provide unprecedented efficiencies and system synergies that are pivotal to the sustainability of massive renewable generation integration. Extension of wholesale high-voltage power markets to allow distribution network connected prosumers to participate, albeit desirable, has stalled on high transaction costs and the lack of a tractable market clearing framework. This paper presents a distributed, massively parallel architecture that enables tractable transmission and distribution locational marginal price (T&DLMP) discovery along with optimal scheduling of centralized generation, decentralized conventional and flexible loads, and distributed energy resources (DERs). DERs include distributed generation; electric vehicle (EV) battery charging and storage; heating, ventilating, and air conditioning (HVAC) and combined heat & power (CHP) microgenerators; computing; volt/var control devices; grid-friendly appliances; smart transformers; and more. The proposed iterative distributed architecture can discover T&DLMPs while capturing the full complexity of each participating DER's intertemporal preferences and physical system dynamics.

KEYWORDS | Distributed power market clearing; distribution network locational marginal prices (DLMP); proximal message passing (PMP); reactive power pricing; reserve pricing

Manuscript received July 10, 2015; revised December 11, 2015; accepted January 8, 2016. Date of publication March 9, 2016; date of current version March 17, 2016. This work was supported in part by the National Science Foundation (NSF) under Grant 1038230.

M. Caramanis and **E. Ntakou** are with Boston University, Boston, MA 02215 USA (e-mail: mcaraman@bu.edu).
W. W. Hogan is with the JFK School of Government, Harvard University, Cambridge, MA 02138 USA.
A. Chakrabortty is with North Carolina State University, Raleigh, NC 27695 USA.
J. Schoene is with Enernex, Knoxville, TN 37932 USA.

Digital Object Identifier: 10.1109/JPROC.2016.2520758

I. INTRODUCTION

A. Background

Vickrey's seminal 1971 work on "Responsive Pricing of Public Utility Services" [12] pioneered extensive work

on short-term marginal-cost-based markets of network delivered commodities and services. Twenty years later, marginal-cost-based wholesale power markets were actually implemented (1990 in England, 1997 in parts of the United States, 1999 in Continental Europe and elsewhere), and are now at the verge of expanding to encompass millions of retail participants connected at medium- and low-voltage distribution network locations. The impetus is provided, among others, by the 2014 NY Department of Public Service (DPS) initiative [137]. Significant embellishments introduced to date in wholesale power markets include: 1) cascaded multiple time-scale markets ranging from 24-h day-ahead markets, to hour-ahead adjustment markets, to 5-min markets; and 2) the simultaneous clearing in these markets of energy as well as the reserves needed to guarantee the power system's integrity in the presence of uncertainty [142], [143].

Meanwhile, technological and manufacturing progress along with climate change concerns [144] are transforming electric power systems with the integration of an increasing share of clean renewable generation whose volatility, lack of active dispatch control, and absence of rotating inertia pose great challenges to the feasibility of efficient, resource-adequate, operationally reliable, and secure power systems. Conventional approaches to meeting these challenges with exclusive reliance on building a stronger transmission and distribution (T&D) infrastructure assisted with more flexible centralized generation (e.g., combined cycle gas turbine (CCGTs)) could fall short of economic and environmental sustainability goals.

Fortunately, a potentially synergistic development has transformed the consumption side of power systems, particularly in the distribution or retail parts of the ledger. Broadly construed distributed energy resources (DERs) connected to primary (9–20 kV) and secondary (120–470 V) voltage feeders are rendering the "pay our light bill" phrase a mere figure of speech with historic origin that goes back more years than we can remember. DERs include, to mention a few, roof top PV, variable speed drives that power HVAC systems with storage like capabilities, plug-in hybrid electric vehicle (PHEV) and EV battery charging with flexible time-shift-able demand, all with volt/var control capable devices, and data centers and computing services with millisecond time-scale power management response capabilities.

The widely discussed hope that DERs can provide the requisite demand response and reserves for economically sustainable massive renewable energy integration has yet materialize. This paper focuses on computation-and-information-sharing barriers that prevent a power-market-based solution. Today's centralized power markets are incomplete; they do not allow for the procurement of reserve services and the commoditization of demand response. New reserve options that do not necessarily mirror conventional generator-provided-reserve dynamics but fit DER capabilities may have to be introduced. The Reg-d secondary reserve introduced recently by PJM is a pioneer in this direction. Of course, new options must be defined equally rigorously (e.g., advanced notice, response ramp, maximum duration of potential provision and the like) and their contribution to system stability needs evaluated thoroughly. Unlike conventional generators, DERs have intertemporally coupled preferences [3], [41] and complex, nonlinear, and often dynamically evolving capabilities [4], [17], [32], [43]. Moreover, existing markets discover clearing prices at high-voltage transmission buses, whereas DERs are connected at medium- to low-voltage distribution feeders where a host of additional costs are present, such as higher line losses, reactive power compensation, and voltage control. In fact, whereas transmission bus locations number in the thousands, associated distribution feeder line buses number in the hundreds of thousands or millions. Finally, the potential provision by DERs of volt/var control services and fast reserves requires significant cyberlayer interaction with the physical power system.

Most importantly, efficient provision of services from DERs requires that DERs can 1) allocate their capacity among real power, reactive power, and reserves at the day-ahead operational planning multiperiod market, and reschedule that allocation at the hour-ahead adjustment market, while 2) being able to deliver the promised services at the much shorter deployment time scales, namely, 5 min for tertiary-like reserves, 4 s for secondary/regulation-like reserves, and real time for primary/frequency-like reserves. Moreover, this must happen in a manner that is consistent with the preference and capability of each DER, and the power system marginal-cost-based dynamic locational prices at each DER distribution bus. Finally, deliverability of scheduled reserves should be certified against voltage constraints at distribution network busses. Existing wholesale power market rules do not allow DERs to reflect their capabilities or intertemporal preferences [3], [17], [41], [42], [61]. Neither existing nor emerging centralized market clearing approaches can be extended to derive the requisite T&D locational marginal prices (T&DLMPs) with acceptable tractability, scalability, and communication requirements, although work pursuing coordination of DERs in large distribution systems has provided useful insights [32]–[34], [137], [138].

It, therefore, comes as no surprise that existing and emerging technologies have focused on DER aggregation (for example, through energy service companies) [48], approximate or time-averaged locational marginal costs, and direct utility demand control based on estimated approximate individual DER information [17], [43], [48]. Recent research has addressed communication and control protocols ranging in bandwidth from very high [direct load control (DLC) of smart appliances by a smart building operator] to low (price signals to request demand response) [39], [40], [59], [81]–[86]. Novel

concepts of packetized energy, with the term referring to temporal quantization into fixed-length intervals of energy utilization by a pool of appliances with common power ratings, especially thermostatic loads, has been introduced and studied with the aim of improving the performance of a building-centered smart microgrid in providing demand response and reducing demand uncertainty [81], [82]. Research on temporally packetized load servicing and research of others on demand response [3], [4], [32], [39], [40], [59] has demonstrated opportunities for reduced aggregate power variability. It has also pointed to a number of operational tradeoffs, including those between the cost of the reduction in aggregate power variability and the length of the mean waiting times (MWTs) of appliances that have queued packet requests [82]; the same applies for the tradeoff between a thermostatic appliance's ability to respond rapidly to a signal calling for demand response and the appliance's capacity to provide sustained response [31]–[33], [55], [62], [63], [83]. Advantages of these approaches are simplicity of transactions and low cost. At the same time, however, they reduce the effective provision of DER reserves since they sacrifice efficiency and consumer acceptance.

B. Overview

This paper presents a distributed cyber–physical system (CPS) architecture intended to realize Fred Schweppe's 1978 visionary "power systems 2000" IEEE SPECTRUM paper [126], and to overcome the limitations of existing and emerging centralized market clearing technologies as well as *ad hoc* partially adapted to global social optimality, localized demand-side management. In particular, its objective is to straddle multiple space and time scales (system-wide, regional, nodal, day-ahead operational planning, hour-ahead adjustment to uncertainty, 5-min economic dispatch, response to 2–4-s regulation signals, and real-time frequency control) while heeding both large physical system integrity requirements (e.g., network topology, key types of regional reserve requirements with prescribed dynamic response capabilities, line flow constraints, and distribution bus voltage limitations) as well as smaller power system component capabilities [e.g., conventional transformers, smart solid-state transformers (SSTs), distributed volt/var control devices, EV, PV, HVAV, and other DERs]. The approach applies directly to modeling frameworks that imply the existence of well-defined market clearing prices, and can support extensions to deal with more general conditions.

In summary, the objective of the proposed distributed CPS architecture is to as follows.

- Co-optimize the allocation of conventional and DER capacity among real power, reactive power, and reserves while enforcing transmission line flow and distribution voltage constraints. Note that since real power, reactive power, and reserves are competing for the same asset capacity, optimal allocation should be consistent with their co-optimization.
- Derive transmission and distribution locational (i.e., bus specific) dynamic marginal prices (T&DLMPs) that are consistent with individual DER capacity allocation optimality, and at the same time, under assumptions of price-taking agents, represent globally competitive prices. We note that, whereas TLMPs together with the much larger set of DLMPs comprise the ensemble of T&DLMPs, the TLMP and DLMP relationship is not trivial. In addition, real power and reactive power affect significantly network-wide costs and constraints, and hence T&DLMPS must reflect broadly construed variable network costs and congestion (e.g., losses, transformer life degradation, line flow, and voltage constraints). We finally note that T&DLMPs reflect demand rationing, whenever relevant, as well as generation and DER marginal opportunity cost. Most importantly, T&DLMPs represent coordinated stable prices resulting from locally interacting decisions, which, nevertheless, propagate to the whole network through iterative proximal message passing (PMP). This observation elevates the objective of distributed/collaborative T&DLMP discovery to a significant challenge raising nontrivial convergence and robustness questions.
- Drill down to the seconds and real time scale to extend capacity allocation scheduling decisions to optimal-feedback closed-loop policies that allow DERs to deploy in real time the reserves promised or scheduled at the hour-ahead or longer time scale. Note that whereas capacity allocation and T&DLMPs are evaluated at the market performance time scale ranging from multiple hours to 5 min, the actual deployment of primary and secondary DER reserves occurs at the real time and 2–4-s time scale, respectively. In conclusion, with the exception of operating reserves which are deployed at the 5-min market time scale, primary and secondary reserve deployment occurs in real time where physical system behavior limitations and capabilities dominate.
- Implement functional interfaces between cyber and physical system layers for all systems or subsystems involved, whether big (the overall transmission or a distribution feeder system) or small [specific DERs and T&D devices such as lines, transformers, smart solid state transformers (SSTs), volt/var control devices such as PV converters–inverters and EV chargers, and the like]. Note that a key characteristic of the proposed CPS framework is the access of the cyber/market-clearing layer to sufficient statistics estimated by

offline studies using physical system models. Examples of such sufficient statistics include:

- zonal reserve requirements $\Re_z$ estimated by offline studies of the grid control physical system;
- the statistics characterizing the stochastic behavior of the regulation signal $y(\tau)$, $t \le \tau \le t+1$, that the grid control system is expected to broadcast at the seconds time scale during hour t;
- the expected intrahour t reserve deployment cost $\vec{J}_b^j(R_b^j(t))$ that DER j located in bus b may expect to incur if it bids $R_b^j(t)$ reserves in the hour-ahead market; $\vec{J}_b^j(R_b^j(t))$ is estimated by using the real-time dynamics of the DER physical system and the statistics of $y(\tau)$;
- develop and implement a dynamic communication architecture protocol that supports the distributed T&DLMP CPS framework allowing bus-specific distributed decisions that meet nodal balances and voltage constraints while also achieving superbus zonal reserve requirements;
- enable dynamic adaptation to grid topology reconfigurations, cyber-attack prevention and recovery, grid islanding contingency planning, and finally post-islanding topology reconfiguration and healthy microgrid operation requirements.

For further elaboration of this paper's context, the reader is referred to Table 1 that places the scope of the proposed CPS distributed architecture framework within the broader power system planning, operation, and security control functions carried out by exercising

Table 1 Power System Centralized and Distributed Cyber and Physical Architecture by Time Scale (Highlighted Cells Represent Components Included in the Proposed CPS Distributed Architecture, and Double Pointed Arrows Their Information Sharing)

	Cyber/ Performance Layer			**Physical Time Differ. Eq.) Layer**	**(Hybrid Discrete Event**
Time \ Scale	**Centralized Decisions**	**Distributed Decisions**	**CS/PS Interf.**	**Centralized/ interconnected**	**Distributed /Individual Agent/microgrid**
Years	**C1,1.**T&D Cap. Expansion	**C1,2.**Generation, DER Capacity Expansion		**P1,1**off line study: -Contingency scen. -Uncertainty Stats	**P1,2.** Off-line study of Annual Costs/Benefits
Months weeks	**C2,1.** Centralized T&D and Generation Maintenance Scheduling	**C2,2.** Distributed, albeit Centrally coordinated, T&D and Generation Maintenance Scheduling		**P2,1**off line studies=> -Types of Reserves (notice, ramp) -Res Req. -Reg. Signal filter $y(t)=\Phi(ACE(t), \Delta\omega(t))$	**P2,2.** Off-line studies on DER Physical Systems to determine Reserve offer Capabilities, Optimal Deployment Policies and Costs, $\vec{J}(R_b^j)$
Days	**C3,1.**Contingency Constrained Unit Commitment, and Transmission Network Connectivity	**C3,2a**-Distr. Net Connectivity when Islanded, **C3,2b** Opt Policy derivtn. for DER Res Depl. and assoc. Av. Costs		**P3,1**off line study of Tr. line flow Cap,, switching stability=> OPF constraints that Stabilize Line Switching	**P3,2.**Offline study. on Stability of Islanded Distr. Feeders/ micro-grids=> micro-grid Reserve Requirements
Hours	**C4,1.** Power, Reserves Capacity Scheduling and load flow => hourly TLMP discovery	**C4,2.**Concurrent Real/ Reactive Power, Reserv. Capacity Scheduling. Line Load flow =>T&DLMP Discovery			**P4,2.** Offline stab. study on microgrid reserve. req. for islanded state frequency control
Minutes to seconds	**C5,1.** Power, Reserves Capacity Scheduling and 5 min gen dispatch => 5 min ex post TLMP discovery and Operational Reserves deployment	**C5,2.**Concurrent Real-Reactive Power, Reserves Scheduling and 5 min ex post T&DLMP Discovery		When Feeder(s)/ Micro-grid Islanded	**P5,2.**Islanded micro-grid controller issued deployment of Regulation Signal
Seconds to Real-Time		**C6,2.**Deployment of DER Regulation Service & Frequency Control Policies		**P6,1**-PMU and Data Gathering, -Automated Switching, -Regulation Signal, $y(t) = \Phi(ACE(t), \Delta\omega(t))$	**P6,2a.**AGC resp. to $y(t)$. Freq. Control resp. to $\Delta\omega_{n(k)}(t)$. **P6,2b.**Policy Driven DER Regulation Service & Freq. Control Depl.

interacting cybersystem (performance) models shown in cells labeled Ci,j and physical system (or interconnected subsystems) models labeled Pi,j. Cyber and physical models are distinguished by their characteristic time scale and their centralized or distributed execution. Physical systems are hybrid continuous-discrete event dynamic systems modeled by differential equations and stochastic process or petri net discrete state transitions. Physical system models are employed in offline and short-horizon look-ahead simulations for contingency planning and feedback control policy design associated with transient, dynamic, and longer term stability management (see [10, pp. 277–280]). Cybersystem models, on the other hand, are used to optimize planning and operational decisions taken centrally, as for example in the centralized clearing of wholesale power markets that schedule energy generation and procure reserves, or decisions taken by individual generators regarding how to bid into the power market. The foundation of our proposed CPS architecture for T&DLMP discovery and DER scheduling is the reliance on distributed decision making using both cyber and physical models along with sufficient statistical inputs from centralized grid control systems.

Highlighted cells in Table 1 show the components of the proposed CPS architecture and their information exchange. In particular, C4,2, C5,2, and P2,2, described in detail in Sections II and III comprise its core. C5.2 with input from P2,2 is the computationally tractable iterative distributed T&DLMP discovery model described in Sections II and III, while P2,2 is the stochastic DP modeling the physical system of DERs which estimate optimal reserve deployment policies for reserve types provided by sufficient statistics communicated by P2,1. DER physical modeling is described in Section V. The rest of the cells of Table 1 depict power system functionality with which the proposed CPS architecture may interface, but we do not discuss or address either the cyber or the physical system models involved in any detail. We instead refer the reader to the rich existing literature in this area. In particular, we assume that investment decisions, maintenance scheduling, unit commitment and transmission network topology, zonal system reserve requirements by reserve type required to meet system stability under key contingencies and renewable penetration, the dynamic properties that each reserve type should be able to satisfy at the real-time deployment time scale (advanced notice, response ramp, duration, and the like), the filter mapping area control error (ACE) and frequency deviations to the broadcast regulation signal, transmission line flow constraints and distribution bus voltage limits, are modeled exogenously, interacting with our proposed CPS architecture through the exchange of sufficient statistics. As already noted, reserve requirements and their dynamic deployment capabilities are sufficient statistics that our CPS architecture imports, while T&DLMP and market clearing trajectories are sufficient statistics that it exports.

The main thrust of our proposed distributed CPS architecture is motivated by the realization that the desired provision of efficient and plentiful reserves from DERs is limited by the inability of existing centrally cleared power markets to address without loss of tractability the often nonlinear and intertemporally coupled DER preferences that correspond to bid structures that are much more complex than the myopic uniform price quantity transactions allowed in current power markets. As a result, existing and emerging centralized power market clearing approaches cannot derive T&DLMPs in a computationally tractable, scalable, and robust manner.

Fig. 1(a) and (b) depicts the overall topology of the meshed transmission and subtransmission power system and the connected radial distribution networks. The main contribution of this paper is the formulation and implementation of a tractable approach to derive real power P, reactive power Q, and reserve RT&DLMPs containing:

- distribution substation DLMPs $\pi_b^P(t), \pi_b^Q(t)\pi_b^R(t)$, including the DLMPs at the transmission/distribution interface bus;
- transmission LMPs $\pi_n^P(t), \pi_n^R(t)$ (note the lack of reactive power LMP).

We propose to continue to model meshed transmission and subtransmission system load flow can be modeled adequately by a simple direct current (dc) approximation which captures transmission line flow capacity congestion and relatively low line losses while disregarding noncompetitive reactive power transactions [23]. For distribution feeders, however, we propose to employ a detailed alternating current (ac) load flow model enabling us to address higher losses [132], transformer variable wear and tear [2], reactive power compensation for line loss mitigation, voltage control and related distribution feeder congestion [129], [145], and DER reserve offer deliver ability [9], [31]. Finally, nonlinear and intertemporally coupled DER preference modeling [3], [4], [17]–[19] is elaborated on in Section V.

Without loss of generality, and in order to improve the readability of the paper, we demonstrate the proposed DLMP discovery approach by focusing on one type of reserves. Additional reserves can be treated similarly, and, in fact, can be modeled more easily, with straightforward simple modifications in the DER reserve constraints. The reserve type we select to model is secondary or regulation reserves, offered in the up and down direction, as is the current practice by PJM and NY ISO market operators. In addition to the increase or decrease of real power output in response to the regulation signal, we describe in Sections II and III how DERs have the additional option to offer reactive power compensation responding similarly to the regulation signal.

Regulation reserves offered to date primarily by centralized generators can be potentially provided by DERs

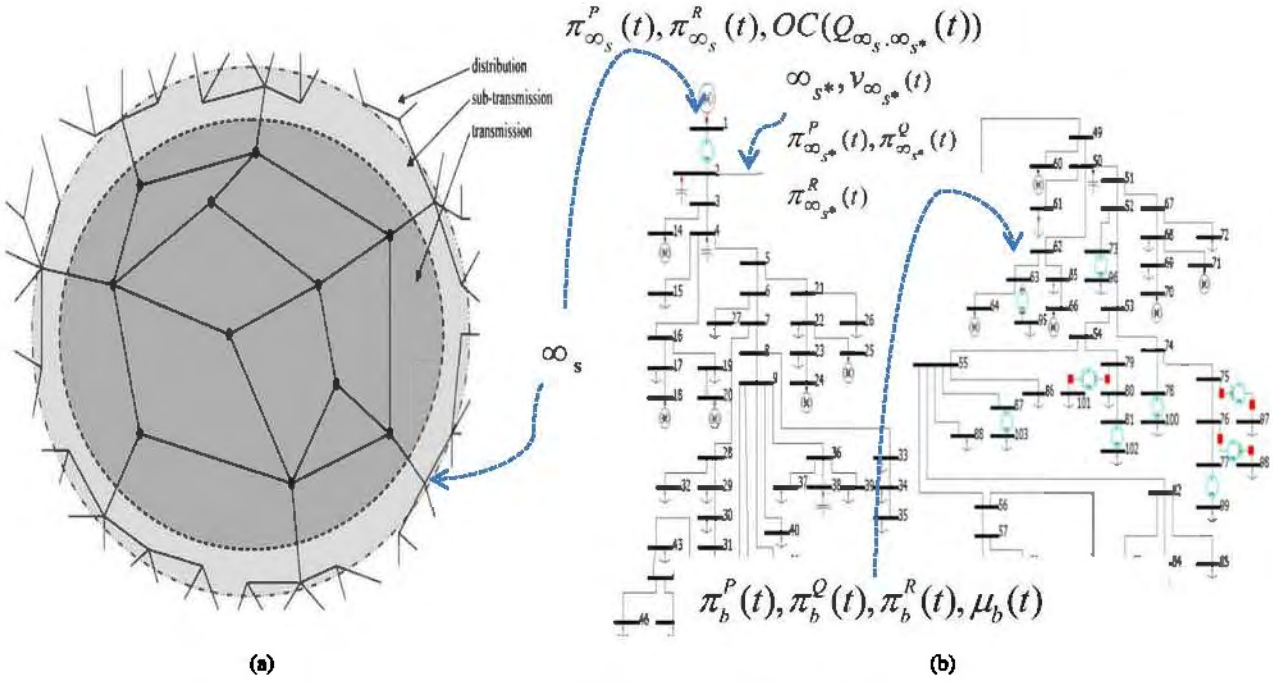

Fig. 1. *(a) Transmission, subtransmission, and distribution schematic. (b) Expanded distribution feeder schematic.*

at a possibly lower cost. With expanding nonrotating renewable generation that lacks inertia, system frequency control that is crucial to the stability of interconnected power systems may benefit from greater availability of fast reserves. Figs. 2 and 3 [138] illustrate how real-time physical power system analysis and observations can capture the impact of increasing nonrotating renewable generation on power system stability. Numerous studies, for example [127], [130], [136], and [146], have reported on the increasing reserve requirements that may become necessary with the massive integration of renewable generation into the grid despite law of large number effects.

The swing equation $H(d\omega(t)/dt) = P_{mech}(t) - P_{elec}(t)$ shows clearly that higher nonrotating generation mix results in lower inertia H and hence larger frequency deviation for the same energy balance disturbance.

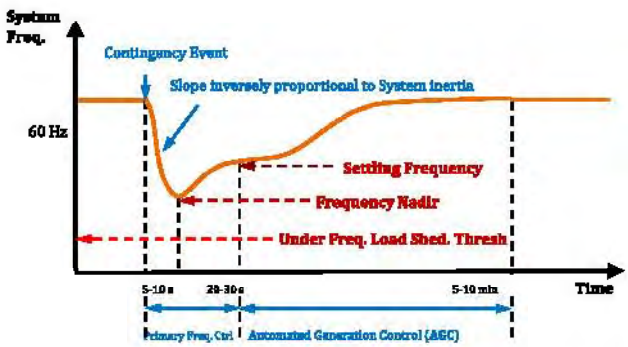

Fig. 2. *System frequency control following a loss-of-generation contingency event.*

The rest of the paper proceeds as follows. Section II defines the problem of scheduling centralized transmission-network-connected and decentralized distribution-network-connected resources to provide optimal real and reactive energy and reserves subject to system and individual resource constraints. The problem is formulated first as a centralized market clearing problem that minimizes social costs, schedules the available capacity of resources, and derives marginal-cost-based T&DLMPs for a day-ahead, hour-ahead, or 5-min real-time market. Although the centralized problem is not tractable, it provides a useful and instructive relationship of DLMPs to the LMPs at the substation interface of distribution and transmission networks. Section III proceeds to describe a tractable and massively parallelizable PMP algorithm consisting of an iterative interaction of DER, line, and bus-specific subproblems that lead to the same solution as the centralized problem. It also discusses the overall architecture's computational and data communication tractability. Section IV argues that the proposed architecture is favorable to cyberattack mitigation, topology control at the operational planning level preceding (albeit interacting with) day-ahead T&DLMP market clearing. It also discusses market implementation issues, possible anomalies, and remedies. Section V describes some representative DERs and the associated CPS subproblems. Section VI presents numerical results, and Section VII concludes and proposes critical future work.

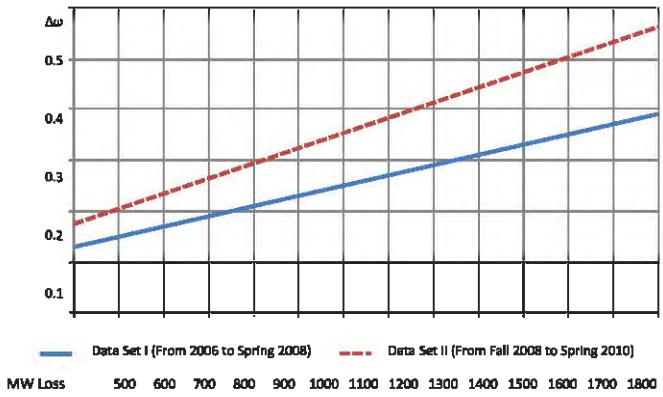

Fig. 3. *Declining grid inertia within ERCOT interconnection from 2006 to 2010. System frequency decline is shown as a function of power loss in the system, with the red curve illustrating the loss of system inertia as a result of increased penetration of renewables.*

II. T&DLMP MARKET CLEARING AS A CENTRALIZED OPTIMIZATION PROBLEM

The capacity scheduling framework presented below presumes the existence of market-clearing prices. More specifically, it presumes that there is a well-defined solution to the associated dual Lagrangian relaxation problem, and there is no duality gap. Subsequent sections address extensions to inherently nonconvex decisions such as unit commitment and network line switching actions that may be guided by T&DLMPs.

A. Notation Summary

A brief notation summary is provided below to assist the reader.

- N^T, N^S, N^z, β^s: Set of 1) transmission buses; 2) distribution substation subtransmission buses; 3) buses in regional reserve zone z; and 4) distribution feeder buses under substation s. $N^S \subset N^T$ and $N^z \subset N^T$.
- $n \in N^T$, $\infty_s \in N^S$, $\infty_{s^*} \in \beta^s$, $b \in \beta^s$, $\phi \in N^T \cup \{\beta^s \forall s \in N^S\}$: 1) typical transmission bus; 2) substation s upstream bus, say at 65 KV, constituting T&D interfaces[1]; 3) substation s downstream bus, say at 11 KV, located directly under the substation main transformer[2]; 4) typical distribution feeder bus; and 5) any bus.
- A_b, H_b: Sets of DERs and distribution lines b, b', connected[3] to bus b.
- $P^j_\phi(t), Q^j_\phi(t), R^j_\phi(t)$: Real power, reactive power, and reserve decisions made at the beginning of period/hour t by market participant j connected to bus ϕ. Note $P_\phi(t) \equiv \sum_j P^j_\phi(t)$ and similarly for $Q_\phi(t), R_\phi(t)$.
- $Q^{j,\mathrm{up}}_\phi(t), Q^{j,\mathrm{dn}}_\phi(t)$: Additional decisions made by DER j connected to bus ϕ. DER j promises to implement these decisions at instances τ and τ' that the regulation signal may take its extreme values $y(\tau) = 1$ and $y(\tau') = -1$.
- $P_{\phi,\phi'}(t), Q_{\phi,\phi'}(t), R_{\phi,\phi'}(t)$: Real power, reactive power, and reserves flowing during period/hour t over line connecting buses ϕ and ϕ' at the end of the line associated with bus ϕ. For example, $P_{n,n'}(t), P_{b,b'}(t)$ denote real power line flows at the end connected to bus n or b, respectively, while $P_{\infty_s\infty_{s^*}}(t)$ is the real power flow from substation s upstream T&D interface bus ∞_s toward the substation-downstream-root-bus ∞_{s^*}.
- Sign convention: An injection or flow into a bus is negative while out of a bus it is positive.[4]
- $v_\phi(t), \ell_{\phi,\phi}(t)$: Voltage square at bus ϕ, and square of current flowing during period/hour t over distribution line connecting buses ϕ, ϕ'.
- up and dn: Superscripts applied to $P_\phi(t)$, $Q_\phi(t)$, $P_{\phi\phi'}(t)$, $Q_{\phi\phi'}(t)$, $\ell_{\phi,\phi'}(t)$, and $v_b(t)$ to represent the bus injections, the resulting line load flow, current, and voltage level at an instance τ that the regulation signal $y(\tau)$ takes its extreme values of $+1$ and -1, respectively. For example, for $y(\tau) = 1$, we have $P^{\mathrm{up}}_b(\tau) = \sum_j (P^j_b(\tau) - R^j_b(\tau))$ at each bus b and reactive power

[1]For simplicity of exposition, we consider that each distribution substation is connected to a single subtransmission bus. This does not lead to any loss of generality, since the relaxation of this assumption leads only to a more complex notation.

[2]Note that line ∞_s, ∞_{s^*} represents the distribution network main transformer and belongs to the distribution network. It connects the feeder root bus ∞_{s^*} to subtransmission bus ∞_s.

[3]Note that H_b essentially describes the distribution network topology.

[4]Real or reactive power generation $P^j_b(t), Q^j_b(t)$ or provision of reserves into bus b, $R^j_b(t)$, is positive, whereas consumption is negative. Similarly, line flows $P_{b,b'}(t), Q_{b,b'}(t), R_{b,b'}(t)$ are positive when the flow is away from b toward b'. Since reserves flow always from bus ∞_{s^*} to bus ∞_s, i.e., they are offered by the distribution network to the transmission network, it is always the case that $R_{\infty_s,\infty_{s^*}}(t) \leq 0$.

injections $Q_b^{up}(\tau) = \sum_j Q_b^{j,up}(\tau)$ which result in $P_{b,b'}^{up}(\tau)$, $Q_{b,b'}^{up}(\tau)$, $\ell_{b,b'}^{up}(\tau)$, $v_b^{up}(\tau)$, and similarly for $y(\tau') = -1$. $R_{b,b'} = (P_{b,b'}^{up}(\tau), P_{b,b'}^{dn}(\tau'))/2$ and $R_{\infty_s,\infty_{s^*}}(t) = (P_{\infty_s,\infty_{s^*}}^{up}(\tau) - P_{\infty_s,\infty_{s^*}}^{dn}(\tau))/2$, are then appropriate relations denoting the flow of reserves over lines b, b' and ∞_s, ∞_{s^*}.

- $X_\phi^j(t); u(X_\phi^j(t)); \bar{J}_\phi^j(R_\phi^j(t))$: 1) State of the energy service[5] received by j during period t; 2) cost (positive) or utility (negative cost) associated with state $X_\phi^j(t)$; and 3) intrahour t reserve deployment cost that j expects[6] to incur if it offers reserves $R_\phi^j(t)$ at the beginning of hour t.
- $\pi_\phi^P(t), (t)\pi_\phi^Q(t), \pi_\phi^{Q,up}(t), \pi_\phi^{Q,dn}(t), \pi_\phi^R(t)$: Real power, reactive power promised during hour t conditional upon $y(t) = 0$, $y(t) = 1$, $y(t) = -1$, respectively, and reserve T&DLMPs at bus ϕ.
- $\mu_b(t), \mu_b^{up}(t), \mu_b^{dn}(t)$: Voltage magnitude constraint dual variables at bus b.
- $v_{b,b'}(t), \mu_{b,b'}(t)$: Voltage square at the end b of line connecting buses b, b', and the corresponding voltage magnitude constraint dual variable. These are quantities estimated by each line in the distributed algorithm. All lines sharing the same bus are induced by regularization terms and dual variable $\varsigma_{b,b'}(t)$ penalizing discrepancies of voltage estimates by lines connected to node b to converge to the same value denoted by $v_b(t)$ and $\mu_b(t) \forall b'$.
- $r_{\phi,\phi'}^t, x_{\phi,\phi'}^t, B_{\phi,\phi'}^t$: Resistance, reactance, and susceptance of line connecting ϕ, ϕ'. Time indexing indicates exogenous dynamic changes in grid topology, ambient temperature, and the like.
- $\Gamma^k(\ell_{b,b'}(t))$: Loss of life of distribution feeder transformer connecting buses b, b'.

B. The Centralized Market Clearing Optimization Problem

As noted in Section I, motivated by the secondary role of losses and reactive power pricing in the transmission (and subtransmission) high-voltage meshed network we use a dc load flow approximation for that portion of the network, while for the distribution feeders we use the relaxed brunch ac load flow model [25]. We proceed with the presentation of:

1) the transmission market model that clears TLMPs (more simply referred to as LMPs) at every bus $n \in N^T$ conditional upon (i.e., given) real power, reactive power,[7] and reserves, $P_{\infty_s,\infty_{s^*}}(t), Q_{\infty_s,\infty_{s^*}}(t), R_{\infty_s,\infty_{s^*}}(t)$, flowing into/from each distribution feeder s at the interface subtransmission bus $\infty_s, \forall s \in N^S \subset N^T$;
2) the distribution market model that clears DLMPs, $\pi_b^P(t), \pi_b^Q(t), \pi_b^R(t) \forall b \in \beta^s$, at each substation s, $\forall s \in N^S \subset N^T$, for given LMPs and reactive power opportunity cost $\pi_{\infty_s}^P(t), \pi_{\infty_s}^R(t)$, $OC(Q_{\infty_s,\infty_{s^*}}(t))$.

Although we present the day-ahead market, the hour-ahead adjustment market and the 5-min real-time markets can be described with straightforward modifications.

1) The Transmission Market LMP Clearing Model: The transmission LMP day-ahead market clearing optimization problem can be written as a loss adjusted shift factor [14] version or a B, θ-based version [10]. The first is generally more efficient, especially under a large number of contingencies [140], while the latter can be easily transformed to a parallelizable distributed PMP algorithm similar to the one presented in Section III.

The shift factor version is formulated first as follows:

$$\min_{P_n^j, R_n^j, \forall j,n,n'} \sum_{j,n,t} \left[u_n^j\left(P_n^j(t)\right) + \bar{J}_n^j\left(R_n^j(t)\right) \right] \tag{A0}$$

subject to constraints associated with dual variables indicated by $\rightarrow$

$$P_n(t) = \sum_j P_n^j(t) \quad P_n^{j\in gen}(t) \geq 0 \quad P_n^{j\in dem}(t) \leq 0$$

$$\sum_n P_n(t) + \text{Losses} = 0 \rightarrow \lambda(t) \qquad \forall t \tag{A1}$$

$$\sum_{j,n\in N^Z,t} R_n^j(t) \geq \Re_Z \rightarrow \pi_Z^R(t) \qquad \forall t \tag{A2}$$

$$\bar{P}_{n,n'}(t) \leq P_{n,n'}^{\text{lin gap}}(t) + \sum_{\hat{n}} P_{\hat{n}}(t) \text{ShF}_{n,n'}^{\hat{n}}(t) \leq \bar{P}_{n,n'}(t)$$
$$\rightarrow \underline{\mu}_{n,n'}(t), \bar{\mu}_{n,n'}(t) \qquad \forall t \tag{A3}$$

$$P_n(t) + \sum_{n'\in H_n} \left[P_{n,n'}^{\text{lin gap}}(t) + \sum_{\hat{n}\in N} P_{\hat{n}}(t) \text{ShF}_{n,n'}^{\hat{n}}(t) \right] = 0$$
$$\rightarrow \pi_n^P(t) \tag{A4}$$

plus capacity constraints, intertemporal coupling such as ramp constraints, and contingency constraints, where $\text{ShF}_{n,n'}^{\hat{n}}(t) \equiv (\partial P_{n,n'}/\partial P_{\hat{n}})$ being the loss adjusted n, n' flow shift factor [14] with respect to injection at bus $\hat{n}$.

The B, θ versions are formulated as

$$\min_{P_n^j, R_n^j, \theta_{n,n'}, \forall j,n,n'} \sum_{j,n,t} u_n^j\left(P_n^j(t)\right) + \sum_{j,n,t} \bar{J}_n^j\left(R_n^j(t)\right) \tag{A5}$$

[5]For example, real power output of a generator, or consumption of an inflexible load $X_b^j(t) = P_b^j(t)$, or an energy service for a flexible load such as inside temperature, battery state of charge, etc., that may depend on current and past consumption $X_b^j(t) = \text{function of } (P_b^j(\tau); \tau \leq t)$.

[6]The expectation is taken over regulation reserve signal trajectory realizations $y(\tau), t \leq \tau \leq t+1$, in an average-cost-stochastic-dynamic-program sense that derives optimal feedback policy response to $y(\tau)$.

[7]We assume that $Q_{\infty_s,\infty_{s^*}}(t)$ flowing from the T&D interface bus ∞_s into the distribution substation downstream bus ∞_{s^*}, takes up a portion of a subtransmission generator's capacity located at bus ∞_s, or close by.

subject to constraints associated with dual variables indicated by $\rightarrow$

$$P_n(t) = \sum_j P_n^j(t) \;\; P_n^{j\in \text{gen}}(t) \geq 0 \quad P_n^{j\in \text{dem}}(t) \leq 0$$

$$\sum_n P_n(t) + \text{Losses} = 0 \;\; \rightarrow \lambda(t) \qquad \forall t \tag{A6}$$

$$\sum_{j,n\in Z,t} R_n^j(t) \geq \Re_Z \;\; \rightarrow \pi_Z^R(t) \qquad \forall t \tag{A7}$$

$$P_{n,n'}(t) = B_{n,n'}(\theta_n(t) - \theta_{n'}(t)) \quad \underline{P}_{n,n'} \leq P_{n,n'}(t) \leq \bar{P}_{n,n'} \;\; \rightarrow \underline{\mu}_{n,n'}(t), \bar{\mu}_{n,n'}(t) \tag{A8}$$

$$\sum_j P_n^j(t) + \sum_{n'\in H_n} P_{n,n'}^j(t) = 0 \;\; \rightarrow \pi_n^P(t) \tag{A9}$$

plus capacity constraints, intertemporal coupling such as ramp constraints, and contingency constraints, with $\theta_n(t)$ the voltage phase difference at bus n relative to the reference bus.

LMP and congestion dual variable relations are obtainable from either version as follows. Forming the Lagrangian and using optimality conditions, we can show that the LMPs satisfy the following relations involving the energy balance and congestion Lagrange multipliers:

$$\pi_{\hat{n}}^P(t) = \lambda(t)\left(1 + \frac{\partial \text{Losses}}{\partial P_{\tilde{g}(\hat{n})}}\right) + \sum_{n,n'} \mu_{n,n'}(t) P_n(t) \text{ShF}_{n,n'}^{\hat{n}}(t)$$

where

$$\mu_{n,n'}(t) \equiv \left[\bar{\mu}_{n,n'}(t) - \underline{\mu}_{n,n'}(t)\right]$$

$$\pi_{\hat{n}}^R(t) = \pi_Z^R(t) = \max_{j,\hat{n}\in Z, R_{\hat{n}}^j > 0} \left[\left|\pi_{\hat{n}}^P(t) - u_{\hat{n}}^j\right| + \frac{\partial \bar{J}_{\hat{n}}^j\left(R_{\hat{n}}^j\right)}{\partial R_{\hat{n}}^j}\right]$$

2) The Distribution Market DLMP Clearing Model: We formulate next the DLMP clearing problem for each distribution network s, using the relaxed brunch ac load flow model [25]. To avoid clatter in the notation, we drop the hour/period reference and the summation over hours in the objective function. The reader can fill those in while benefiting from the simplified notation.

a) Objective function: Reactive power, equipment life degradation, and voltage control introduce additional terms in the objective function relative to the transmission problem, and, of course, additional decision variables. More specifically, the objective function[8] includes the following six terms described first in words in the order that they appear in the mathematical formulas that follow.

- The cost or (negative) utility of DER j associated with achieving state X.
- The expected intrahour t deployment cost for reserves $R_b^j(t)$ promised by j in hour t.
- The cost of procuring real power $P_{\infty_s,\infty_{s^*}}$ from the wholesale transmission market.
- The opportunity cost incurred by a centralized generator with capacity C_{∞}, that is closest to the substation bus and is responsible for compensating reactive power $Q_{\infty_s,\infty_{s^*}}$ flowing into ∞_s. Note that $\pi_{\infty_s}^{OC}$ is the marginal opportunity cost to that generator associated with foregoing the use of a unit of real power production for the provision of reactive power. This is either the difference of the real power LMP and the generator's variable cost, or the LMP of reserves that the generator has to forgo from offering. This opportunity cost is equivalent to a reactive power LMP at the subtransmission bus ∞_s

$$\pi_{\infty_s}^Q(t) \equiv \pi_{\infty_s}^{OC} \frac{\partial\left(C_{\infty_s} - \sqrt{C_{\infty_s}^2 - Q_{\infty_s,\infty_{s^*}}^2}(t)\right)}{\partial Q_{\infty_s,\infty_{s^*}}(t)}.$$

  An important point here is that whereas $\pi_{\infty_s}^P(t)$ and $\pi_{\infty_s}^R(t)$ are dependent on the transmission market's reaction to distribution network demand, $\pi_{\infty_s}^Q(t)$ is an explicit function of distribution feeder decisions that determine $Q_{\infty_s,\infty_{s^*}}(t)$.
- The negative of the income[9] made by selling reserves to the wholesale market. Recall that DERs can promise reserves and reactive power whose deployment depends linearly on the regulation signal $y(\tau) \in [0,1]$ for each $\tau \in [t, t+1]$. The associated maximal flow of the bidirectional reserves considered here equals one half of the real power flow difference during instances τ and τ', when $y(\tau) = 1$ and $y(\tau') = -1$. Denoting these instances and the associated load flow by superscripts up and dn, we quantify the flow of reserves over line b, b' as $R_{b,b'}(t) = (P_{b,b'}^{\text{up}}(t) - P_{b,b'}^{\text{dn}}(t))/2$. Following our sign convention, $R_{b,b'}(t)$ is negative if reserves flow from bus b' to bus b; positive otherwise. Hence, $R_{\infty_s,\infty_{s^*}}$ is negative and the value of providing these reserves to the T&D interface bus ∞_s is $-\pi_{\infty_s}^R R_{\infty_s,\infty_{s^*}} = -\pi_{\infty_s}^R (P_{\infty_s,\infty_{s^*}}^{\text{up}} - P_{\infty_s,\infty_{s^*}}^{\text{dn}})/2$. This value (or income to the distribution network) is subtracted from the objective function costs which are minimized.
- The cost of substation voltage deviations from its nominal value.

[8]Note that time indexing and summation over time are implicit and not shown to simplify the notation.

[9]Recall $R_{\infty_s,\infty_{s^*}} \leq 0$ since flow is from ∞_{s^*} to ∞_s.

— The cost of life loss of transformers loaded close to or beyond their rated capacity.
— To focus the contribution of $Q_b^{j,\mathrm{up}}(t)$ and $Q_b^{j,\mathrm{dn}}(t)$ on the avoidance of voltage magnitude constraint violations that would deter the deliverability of reserves, a regularization term is added to incent optimal $Q_b^{j,\mathrm{up}}(t)$ and $Q_b^{j,\mathrm{dn}}(t)$ to differ from $Q_b^j(t)$ primarily for the purpose of voltage constraint related deliverability of reserves.

The above objective function is representative rather than exhaustive or free from approximations. Nevertheless, it can be easily refined at will. For example, transformer life degradation $\Gamma(\ell_{b,b'}(t))$ may be modeled more as a function of $\ell_{b,b'}(t)$, the ambient temperature $\theta(t)$, and the transformer's hottest spot temperature at the beginning of hour t, $\theta_{b,b'}^{\text{hottest spot}}(t-1)$. Also, additional components may be introduced such as the efficiency loss in electric energy conversion to energy service (for example, refrigeration) due to voltage levels deviating from optimal levels for which appliances have been designed, loss of real power associated to the provision of reactive power, and potentially others, such as transformer tap changers. Although such extensions burden further the computational tractability of the centralized problem, they are easy to handle through the distributed architecture developed in Section III.

b) Three sets of load flow balance equations and voltage constraints yield $\pi_b^P(t)$, $\pi_b^Q(t)$, $\pi_b^R(t)$, $\pi_b^{Q,\mathrm{up}}(t)$, $\pi_b^{Q,\mathrm{dn}}(t)$, $\mu_b(t)$, $\mu_b^{\mathrm{up}}(t)$, *and* $\mu_b^{\mathrm{dn}}(t)$: Note that reactive power compensation does not only affect line losses and transformer life degradation, but also voltage magnitudes. If voltage magnitude constraints become binding under a reserve deployment request, the deliverability of reserves may be affected. Since reactive power compensation can mitigate voltage constraints, delivering it in response to reserve deployment request levels provides an additional means for enabling the deliverability of reserves. To this end, three reactive power decisions are made for each of the three key instances of regulation signal values $y(\tau)=1$, $y(\tau')=-1$, and $y(\tau'')=0$. These decisions allow us to express real and reactive power injections for any intermediate value of y as convex combinations of the three key instances as linear functions[10] of the decision variables $P_b^j(t)$, $R_b^j(t)$, $Q_b^j(t)$, $Q_b^{j,\mathrm{up}}(t)$, and $Q_b^{j,\mathrm{dn}}(t)$. In particular, recalling that the sign convention represents bus injections as negative quantities, we have

$$
\begin{aligned}
& P_b^{j,y}(\tau) = P_b^j(t) - y(\tau)R_b^j(t) \\
\Rightarrow\ & P_b^{j,\mathrm{up}}(t) = P_b^j(t) - R_b^j(t);\ P_b^{j,\mathrm{dn}}(t) = P_b^j(t) + R_b^j(t) \\
& Q_b^{j,y}(\tau) = Q_b^j(t) + 1_{y(\tau)>0}\, y(\tau)\left(Q_b^{j,\mathrm{up}}(t) - Q_b^j(t)\right) \\
& \qquad + 1_{y(\tau)<0}\, y(\tau)\left(Q_b^j(t) - Q_b^{j,\mathrm{dn}}(t)\right).
\end{aligned}
$$

[10]This linearity maintains feasibility since the resulting P, Q operating point is inside the capacity circle.

The purpose of decision variables $Q_b^{j,\mathrm{up}}(t)$ and $Q_b^{j,\mathrm{dn}}(t)$, which are rewarded by prices $\pi_b^{Q,\mathrm{up}}$ and $\pi_b^{Q,\mathrm{dn}}$, is to enable the deliverability of secondary reserves, i.e., to allow reserves offered at distribution network buses to maximize $R_{\infty_{s'},\infty_s} = (P^{\mathrm{up}}_{\infty_{s'},\infty_s} - P^{\mathrm{dn}}_{\infty_{s'},\infty_s})/2$ and reach the substation transmission/distribution interface bus ∞_s without violating voltage magnitude constraints.

Omitting time arguments for notational simplicity, we write the three sets of load flow and voltage constraints associated with dual variables indicated by $\rightarrow$, as follows:

$$\sum_{j\in A_b} P_b^j + \sum_{b'\in H_b} P_{b,b'} = 0 \rightarrow \pi_b^P \tag{B1}$$

$$\sum_{j\in A_b}\left[P_b^j - R_b^j\right] + \sum_{b'\in H_b} P_{b,b'}^{\mathrm{up}} = 0 \tag{B2}$$

$$\sum_{j\in A_b}\left[P_b^j + R_b^j\right] + \sum_{b'\in H_b} P_{b,b'}^{\mathrm{dn}} = 0 \tag{B3}$$

$$\sum_{j\in A_b} Q_b^j + \sum_{b'\in H_b} Q_{b,b'} = 0 \rightarrow \pi_b^Q \tag{B4}$$

$$\sum_{j\in A_b} Q_b^{j,\mathrm{up}} + \sum_{b'\in H_b} Q_{b,b'}^{\mathrm{up}} = 0 \rightarrow \pi_b^{Q,\mathrm{up}}$$

$$\sum_{j\in A_b} Q_b^{j,\mathrm{dn}} + \sum_{b'\in H_b} Q_{b,b'}^{\mathrm{dn}} = 0 \rightarrow \pi_b^{Q,\mathrm{dn}} \tag{B5}$$

$$R_{b,b'} \equiv \frac{\left(P_{b,b'}^{\mathrm{up}} - P_{b,b'}^{\mathrm{dn}}\right)}{2}$$

$$\sum_{j\in A_b} R_b^j + \sum_{b'\in H_b} R_{b,b'} = 0 \rightarrow \pi_b^R \tag{B6}$$

$$\ell_{b,b'} = \frac{\left\{(P_{b,b'})^2 + (Q_{b,b'})^2\right\}}{v_b} \tag{B7}$$

$$\ell_{b,b'}^{\mathrm{up}} = \frac{\left\{\left(P_{b,b'}^{\mathrm{up}}\right)^2 + \left(Q_{b,b'}^{\mathrm{up}}\right)^2\right\}}{v_b^{\mathrm{up}}}$$

$$\ell_{b,b'}^{\mathrm{dn}} = \frac{\left\{\left(P_{b,b'}^{\mathrm{dn}}\right)^2 + \left(Q_{b,b'}^{\mathrm{dn}}\right)^2\right\}}{v_b^{\mathrm{dn}}} \tag{B8}$$

$$v_{b'} = v_b - 2\left(r_{b,b'}P_{b,b'} + x_{b,b'}Q_{b,b'}\right) + \left(r_{b,b'}^2 + x_{b,b'}^2\right)\ell_{b,b'} \tag{B9}$$

$$v_{b'}^{\mathrm{up}} = v_b^{\mathrm{up}} - 2\left(r_{b,b'}P_{b,b'}^{\mathrm{up}} + x_{b,b'}Q_{b,b'}^{\mathrm{up}}\right) + \left(r_{b,b'}^2 + x_{b,b'}^2\right)\ell_{b,b'}^{\mathrm{up}}$$

$$v_{b'}^{\mathrm{dn}} = v_b^{\mathrm{up}} - 2\left(r_{b,b'}P_{b,b'}^{\mathrm{dn}} + x_{b,b'}Q_{b,b'}^{\mathrm{dn}}\right) + \left(r_{b,b'}^2 + x_{b,b'}^2\right)\ell_{b,b'}^{\mathrm{dn}} \tag{B10}$$

$$P_{b,b'} + P_{b',b} = r_{b,b'}\ell_{b,b'} \tag{B11}$$

$$P_{b,b'}^{\mathrm{up}} + P_{b',b}^{\mathrm{up}} = r_{b,b'}\ell_{b,b'}^{\mathrm{up}};\ P_{b,b'}^{\mathrm{dn}} + P_{b',b}^{\mathrm{dn}} = r_{b,b'}\ell_{b,b'}^{\mathrm{dn}} \tag{B12}$$

$$Q_{b,b'} + Q_{b',b} = x_{b,b'}\ell_{b,b'} \tag{B13}$$

$$Q_{b,b'}^{\mathrm{up}} + Q_{b',b}^{\mathrm{up}} = x_{b,b'}\ell_{b,b'}^{\mathrm{up}};\ Q_{b,b'}^{\mathrm{dn}} + Q_{b',b}^{\mathrm{dn}} = x_{b,b'}\ell_{b,b'}^{\mathrm{dn}} \tag{B14}$$

$$\underline{v} \le v_b \le \bar{v} \rightarrow \underline{\mu}_b, \bar{\mu}_b \quad \mu_b \equiv \bar{\mu}_b - \underline{\mu}_b \tag{B15}$$

$$\underline{v} \le v_b^{\mathrm{up}} \le \bar{v} \rightarrow \underline{\mu}_b^{\mathrm{up}}, \bar{\mu}_b^{\mathrm{up}} \quad \mu_b^{\mathrm{up}} \equiv \bar{\mu}_b^{\mathrm{up}} - \underline{\mu}_b^{\mathrm{up}} \tag{B16}$$

$$\underline{v} \le v_b^{\mathrm{dn}} \le \bar{v} \rightarrow \underline{\mu}_b^{\mathrm{dn}}, \bar{\mu}_b^{\mathrm{dn}} \quad \mu_b^{\mathrm{dn}} \equiv \bar{\mu}_b^{\mathrm{dn}} - \underline{\mu}_b^{\mathrm{dn}}. \tag{B17}$$

We note briefly that the nonlinear equality constraints (B7) and (B8) impose nonconvexities which have been studied extensively by Javad Lavaei, Steven Low and collaborators [6], [9], [27–29], [50]. It generally turns out that these nonconvexities can be relaxed under mild conditions without loss of optimality in radial networks as is the case with distribution feeders. This is one of the reasons why linear dc load flow approximations continue to comprise a desirable option for modeling meshed high-voltage transmission network load flow.

c) DER specific constraints and state dynamics: DERs can allocate their capacity C_b^j to real and reactive power (e.g., PV and other power electronics equipped devices) or to real and reactive power and reserves (e.g., EV, distributed microgenerators). Inflexible loads, on the other hand, cannot provide reserves and consume reactive power according to a fixed load factor. Universal constraints that DERs must observe when they provide bidirectional secondary reserves include

$$\begin{aligned} & R_b^j \le \min\left(P_b^j, C_b^j - P_b^j\right) \\ & \left(P_b^j\right)^2 + \left(Q_b^j\right)^2 \le \left(C_b^j\right)^2 \\ & \left(P_b^j - R_b^j\right)^2 + \left(Q_b^{j,\mathrm{up}}\right)^2 \le \left(C_b^j\right)^2 \\ & \left(P_b^j + R_b^j\right)^2 + \left(Q_b^{j,\mathrm{dn}}\right)^2 \le \left(C_b^j\right)^2. \end{aligned}$$

In addition, DER state dynamics and constraints are relevant in the multiperiod day-ahead markets. For example, as discussed in greater detail in Section IV, the dynamics of the state of charge of an EV battery $X_b^j(t)$ are generally represented by

$$X_b^j(t) = f\left(X_b^j(t-1), P_b^j(t)\right).$$

d) DLMP components and DLMP relation to LMPs: Forming the Lagrangian of the DLMP market clearing minimization problem and utilizing optimality conditions, it is possible [2] to determine generally instructive, and, as it turns out, useful relations between LMPs and DLMPs. In particular, the DLMP building blocks and their relationship to LMPs is shown below with hatted ^ variables representing a cost-free resource at bus b.

- For real power

$$\pi_b^P = \begin{cases} \pi_{\infty_s}^P \dfrac{\partial P_{\infty_s,\infty_{s*}}}{\partial \hat{P}_b} + \dfrac{\pi_{\infty_s}^{\mathrm{QC}} Q_{\infty_s,\infty_{s*}}}{\sqrt{C_{\infty_s}^2 - Q_{\infty_s,\infty_{s*}}^2}} \dfrac{\partial Q_{\infty_s,\infty_{s*}}}{\partial \hat{P}_b} \\ + \sum\limits_{b'} \mu_{b'} \dfrac{\partial v_{b'}}{\partial \hat{P}_b} + \sum\limits_{\hat{b},\hat{b}' \in tr} \dfrac{\partial \Gamma(\ell_{\hat{b},\hat{b}'})}{\partial \hat{P}_b}. \end{cases}$$

- For reactive power

$$\pi_b^Q = \begin{cases} \pi_{\infty_s}^P \dfrac{\partial P_{\infty_s,\infty_{s*}}}{\partial \hat{Q}_b} + \dfrac{\pi_{\infty_s}^{\mathrm{QC}} Q_{\infty_s,\infty_{s*}}}{\sqrt{C_{\infty_s}^2 - Q_{\infty_s,\infty_{s*}}^2}} \dfrac{\partial Q_{\infty_s,\infty_{s*}}}{\partial \hat{Q}_b} \\ + \sum\limits_{b'} \mu_{b'} \dfrac{\partial v_{b'}}{\partial \hat{Q}_b} + \sum\limits_{\hat{b},\hat{b}' \in tr} \dfrac{\partial \Gamma(\ell_{\hat{b},\hat{b}'})}{\partial \hat{Q}_b}. \end{cases}$$

- For reactive power promised under the $y = 1$ contingency

$$\pi_b^{Q,\mathrm{up}} = \frac{\pi_{\infty_s}^R}{2} \frac{\partial P_{\infty_s,\infty_{s*}}^{\mathrm{up}}}{\partial \hat{Q}_b^{\mathrm{up}}} + \sum_{b'} \mu_{b'}^{\mathrm{up}} \frac{\partial v_{b'}^{\mathrm{up}}}{\partial \hat{Q}_b^{\mathrm{up}}}.$$

- For reactive power promised under the $y = -1$ contingency

$$\pi_b^{Q,\mathrm{dn}} = -\frac{\pi_{\infty_s}^R}{2} \frac{\partial P_{\infty_s,\infty_{s*}}^{\mathrm{dn}}}{\partial \hat{Q}_b^{\mathrm{dn}}} + \sum_{b'} \mu_{b'}^{\mathrm{dn}} \frac{\partial v_{b'}^{\mathrm{dn}}}{\partial \hat{Q}_b^{\mathrm{dn}}}.$$

- For reserves

$$\pi_b^R = \pi_{\infty_s}^R \frac{\partial R_{\infty_s,\infty_{s*}}}{\partial \hat{R}_b} + \sum_{b'} \mu_{b'}^{\mathrm{up}} \frac{\partial v_{b'}^{\mathrm{up}}}{\partial \hat{R}_b} + \sum_{b'} \mu_{b'}^{\mathrm{dn}} \frac{\partial v_{b'}^{\mathrm{dn}}}{\partial \hat{R}_b}$$

where $R_{\infty_s,\infty_{s*}} = \left(P_{\infty_s,\infty_{s*}}^{\mathrm{up}} - P_{\infty_s,\infty_{s*}}^{\mathrm{dn}}\right)/2$.

The above relations can provide a significant speedup in the accuracy and convergence of DLMPs estimated iteratively in the massively parallel distributed PMP dual decomposition algorithm proposed in Section III. Indeed, Ntakou and Caramanis [125] show how the relations above can be used to improve the accuracy of inequality dual variables μ_b which converge at a significantly slower rate than equality constraint dual variables. In [125], the authors show that a filter can be constructed using the above DLMP relations to 1) improve the accuracy of μ_b estimates by imposing consistency to the above relations in which μ_b is over determined; and 2) even more interestingly, feed the improved μ_b estimates back to improve the DLMP accuracy. Periodic implementation of this filter has the potential to enhance the overall convergence rate of the distributed DLMP clearing algorithm.

III. T&DLMP MARKET CLEARING AS A DISTRIBUTED DUAL DECOMPOSITION OPTIMIZATION PROBLEM

This section presents a distributed CPS architecture framework that overcomes existing power market computational tractability and information communication limitations to derive 1) dynamic T&DLMPs, at distribution network buses $\pi_b^P(t)$, $\pi_b^Q(t)$, $\pi_b^{Q,\mathrm{up}}(t)$, $\pi_b^{Q,\mathrm{dn}}(t)$, and $\pi_b^R(t)$, including the upstream substation bus $\pi_{\infty_s}^P(t)$, $\pi_{\infty_s}^Q(t)$, $\pi_{\infty_s}^R(t)$ at the interface with the transmission network, and transmission buses $\pi_n^P(t)$ and $\pi_n^R(t)$; and 2) the corresponding primal decisions that schedule the capacity of connected devices at the distribution, transmission/distribution interface, and transmission busses $P_b^j(t)$, $Q_b^j(t)$, $Q_b^{\mathrm{up},j}(t)$, $Q_b^{\mathrm{dn},j}(t)$, $R_b^j(t)$; $P_{\infty_s}^j(t)$, $Q_{\infty_s}^j(t)$, $R_{\infty_s}^j(t)$; and

$P_n^j(t)$, $R_n^j(t)$. Our CPS architecture relies on an iterative approach with fully distributed decision making. As such, it is scalable to increasing the number of buses and DERs. Distributed decision making allows the inclusion of DERs with complex dynamics and intertemporal preferences. We employ a communication architecture that is based on information passed only to proximal buses. Convergence can be also certified through PMP which increases trivially the number of iterations needed to certify convergence by an increment that is proportional to the depth of distribution feeders [5].

As we describe below, the proposed distributed T&D market clearing architecture relies on a broadly construed price directed decomposition process where participating agents make converging iterative decisions on 1) bus-specific dual variables, i.e., nodal price discovery of real and reactive power and reserves; and 2) device-specific primary variables, i.e., allocation of generator/load/DER capacity to real power, reactive power and reserves, and determination of line (and or transformer) flows, losses, life loss, and voltage magnitudes at their beginning and ending buses. Nodal decisions determine prices consistent with nodal imbalances and make them available to connected/proximal devices. During the iterative convergence process, devices observe price estimates at their connection bus(es) and update injections/withdrawals and flows modifying the nodal balance. Line/transformer devices are connected to two buses, while generator/load/DER devices are connected to a single bus. Bus-specific price decisions coordinate the decisions of connected devices. The parsimonious, i.e., proximal communication of information to directly connected buses, and the fully distributed iterative decision making render the proposed CPS architecture tractable and scalable, while at the same time enforcing the consistency of nodal prices and devices across the whole network. The distributed architecture is equally applicable to all three cascaded market time scales including the day-ahead multiperiod operational planning market, the hour-ahead adjustment market, and the 5-min market.

The bus- and device-specific decision agents described above iterate for a given T&D network topology and centralized generation unit commitment. It is noteworthy that device decision agents—particularly key DER decision agents—are associated with preferences and real-time dynamics whose modeling at the market/cyber time scale require estimates of finer real-time deployment costs $\bar{J}_b^j(R_b^j(t), P_b^j(t), X_b^j(t))$ that are expected to be incurred during the real-time-scale deployment of reserves which is yet unknown at the market clearing time scale. Therefore, for market time-scale decisions, DERs require estimates of the relevant expected intrahour t reserve deployment cost. In our distributed CPS framework, these estimates will be generally provided by the solution of an embedded stochastic DP problem. An interface with the physical DER system dynamics and capabilities is required to model and solve this DP problem. The same DP problem solution, in addition to providing $\bar{J}$ required at the market clearing time scale, determines also the optimal feedback policy for use during reserve deployment.

A. The Proposed Distributed T&DLMP Market Clearing CPS Architecture

We build on extensive Lagrangian relaxation work specialized to robust and tractable versions of PMP algorithms [20] including alternating direction method of multipliers (ADMM) algorithms by Kranning [1], predictor corrector proximal multiplier (PCPM) in [9], and others [26], [29], [32], [43] that are applicable to our proposed distributed CPS architecture framework. These algorithms can handle convex relaxation ac load flow modeling. Fig. 4 depicts an illustrative three-bus network with three line devices and five generator/loads/DER devices connected to these buses. As such, Fig. 4 elaborates the notion of single-bus and two-bus connected devices. We proceed to describe our Lagrangian-relaxation-genre PMP algorithm. More specifically, we describe a novel architecture that synthesizes individual bus decisions and energy balance with super bus decisions and reserve requirement constraints that are consistent with T&DLMP distribution feeder-wide reserve deliverability constraints and clearing of reserve requirements on a zonal/regional basis. The current practice of not pricing reactive prices in pure transmission buses is retained in the proposed architecture.[11] The following iterative steps where k, $k+1, \ldots$, denote the current and next iteration, describe the proposed architecture.

We use $\hat{}$ to denote estimates after the end of iteration k, and remind the reader that $v_{b,b'}(t)$ is defined as the voltage square at the end b of the line connecting buses b, b', while $\mu_{b,b'}(t)$ is the corresponding voltage magnitude constraint dual variable. Omitting for notational simplicity the time designation and summation over the hours of the day-ahead market, we describe the distributed algorithm as the iterative execution of the following three steps whose output is marked by an iteration $k+1$ superscript. Iteration $k+1$ starts after the DLMP revision that occurred after the end of iteration k. More specifically, device subproblems resolve as soon as they receive updated DLMPs.

[11]This is not a necessary restriction. It can be relaxed with no major impact on the computational tractability of estimating reactive power marginal costs at transmission buses. By retaining this current practice we simply start with minimal change in the current whole sale power market rules where reactive power is not priced dynamically, in order to 1) save on transaction costs and 2) in recognition that reactive power provision in the transmission network is associated with local market power due to the fact that reactive power does not travel far without incurring very significant losses.

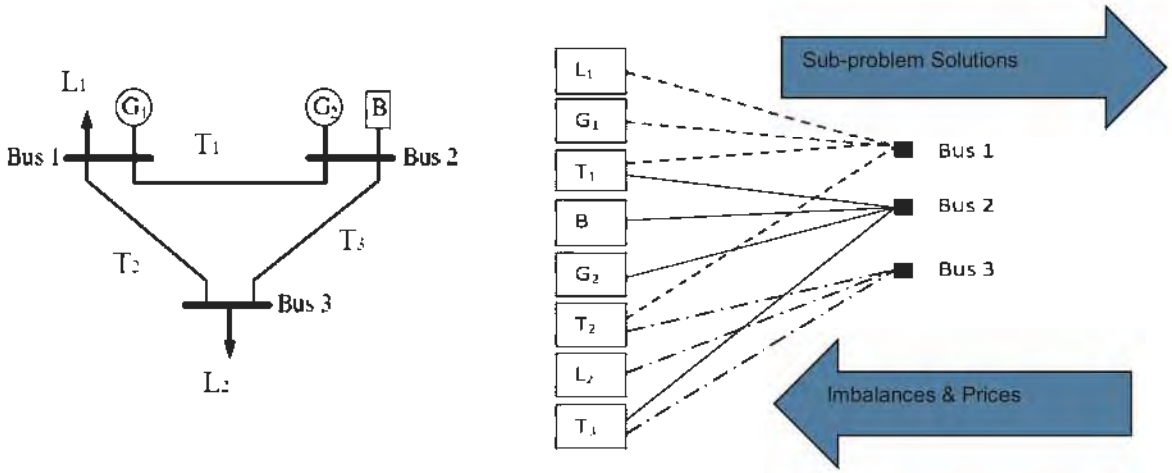

Fig. 4. *PMP algorithm.*

Otherwise they remain idle. The three iteration steps are described next.

- Single-bus-connected devices solve asynchronously the following subproblem:

$$\min_{P_b^j,R_b^j,Q_b^j,Q_b^{j,\mathrm{up}},Q_b^{j,\mathrm{dn}}} u_b^j\left(X_b^j\right)+\vec{J}_b^j\left(R_b^j\right)+\hat{\pi}_b^{P,k}P_b^{j,k}+\hat{\pi}_b^{Q,k}Q_b^{j,k}-\hat{\pi}_b^{R,k}R_b^{j,k}+\hat{\pi}_b^{Q,\mathrm{up},k}Q_b^{j,\mathrm{up},k}+\hat{\pi}_b^{Q,\mathrm{dn},k}Q_b^{j,\mathrm{up},k}+\text{iteration } k+1 \text{ regularization terms}$$

subject to device specific constraints.

- Two-bus-connected devices (lines and transformers, including line $\infty_s, \infty_{s'}$) resolve the following subproblem[12] as soon as they receive the kth iteration DLMPs from buses b and b'

$$\min_{P_{b,b'},P_{b',b}^y,P_{b',b}^y,P_{b',b},Q_{b,b'},Q_{b',b},Q_{b,b'}^y,Q_{b',b}^y,v_{b,b'},v_{b',b},v_{b,b'}^y,v_{b',b}^y;y=\mathrm{up,dn}}$$

$$\hat{\pi}_b^{P,k}P_{b,b'}+\hat{\pi}_b^{R,k}\frac{P_{b,b'}^{\mathrm{up}}-P_{b,b'}^{\mathrm{dn}}}{2}+\hat{\pi}_b^{Q,k}Q_{b,b'}+\hat{\pi}_{b'}^{P,k}P_{b',b}+\hat{\pi}_{b'}^{R,k}\frac{P_{b',b}^{\mathrm{up}}-P_{b',b}^{\mathrm{dn}}}{2}+\hat{\pi}_{b'}^{Q,k}Q_{b',b}+\sum_{y=\mathrm{up,dn}}\left\{\hat{\pi}_b^{Q,y,k}Q_{b,b'}^y+\hat{\pi}_{b'}^{Q,y,k}Q_{b',b}^y\right\}+\varsigma_{b,b'}^k v_{b,b'}+\varsigma_{b',b}^k v_{b',b}+\sum_{y=\mathrm{up,dn}}\left\{\varsigma_b^{y,k}v_{b,b'}^y+\varsigma_{b'}^{y,k}v_{b',b}^y\right\}$$

+ iteration $k+1$ regularization terms enforcing, amongst others, consistency of voltage levels estimated by each line connected to bus b involving the estimate of $\hat{\mu}_b^k, \hat{\mu}_b^k$ (see [5] and [125]), subject to constraints associated with dual variables indicated by $\rightarrow$

$$\ell_{b,b'}\geq\frac{\left\{(P_{b,b'})^2+(Q_{b,b'})^2\right\}}{v_{b,b'}}$$

$$\ell_{b,b'}^{\mathrm{up}}\geq\frac{\left\{\left(P_{b,b'}^{\mathrm{up}}\right)^2+\left(Q_{b,b'}^{\mathrm{up}}\right)^2\right\}}{v_{b,b'}^{\mathrm{up}}}$$

$$\ell_{b,b'}^{\mathrm{dn}}\geq\frac{\left\{\left(P_{b,b'}^{\mathrm{dn}}\right)^2+\left(Q_{b,b'}^{\mathrm{dn}}\right)^2\right\}}{v_{b,b'}^{\mathrm{dn}}}$$

$$v_{b',b}=v_{b,b'}-2\left(r_{b,b'}P_{b,b'}+x_{b,b'}Q_{b,b'}\right)+\left(r_{b,b'}^2+x_{b,b'}^2\right)\ell_{b,b'}$$

$$v_{b',b}^{\mathrm{up}}=v_{b,b'}^{\mathrm{up}}-2\left(r_{b,b'}P_{b,b'}^{\mathrm{up}}+x_{b,b'}Q_{b,b'}^{\mathrm{up}}\right)+\left(r_{b,b'}^2+x_{b,b'}^2\right)\ell_{b,b'}^{\mathrm{up}}$$

$$v_{b',b}^{\mathrm{dn}}=v_{b,b'}^{\mathrm{up}}-2\left(r_{b,b'}P_{b,b'}^{\mathrm{dn}}+x_{b,b'}Q_{b,b'}^{\mathrm{dn}}\right)+\left(r_{b,b'}^2+x_{b,b'}^2\right)\ell_{b,b'}^{\mathrm{dn}}$$

$$P_{b,b'}+P_{b',b}=r_{b,b'}\ell_{b,b'}$$

$$P_{b,b'}^{\mathrm{up}}+P_{b',b}^{\mathrm{up}}=r_{b,b'}\ell_{b,b'}^{\mathrm{up}}$$

$$P_{b,b'}^{\mathrm{dn}}+P_{b',b}^{\mathrm{dn}}=r_{b,b'}\ell_{b,b'}^{\mathrm{dn}}$$

$$Q_{b,b'}+Q_{b',b}=x_{b,b'}\ell_{b,b'}$$

$$Q_{b,b'}^{\mathrm{up}}+Q_{b',b}^{\mathrm{up}}=x_{b,b'}\ell_{b,b'}^{\mathrm{up}}$$

$$Q_{b,b'}^{\mathrm{dn}}+Q_{b',b}^{\mathrm{dn}}=x_{b,b'}\ell_{b,b'}^{\mathrm{dn}}$$

$$\underline{v}\leq v_{b,b'}\leq\bar{v}\rightarrow\mu_{b,b'}$$

$$\underline{v}\leq v_{b,b'}^{\mathrm{up}}\leq\bar{v}\rightarrow\mu_{b,b'}^{\mathrm{up}}$$

$$\underline{v}\leq v_{b,b'}^{\mathrm{dn}}\leq\bar{v}\rightarrow\mu_{b,b'}^{\mathrm{dn}}$$

$$\underline{v}\leq v_{b',b}\leq\bar{v}\rightarrow\mu_{b',b}$$

$$\underline{v}\leq v_{b',b}^{\mathrm{up}}\leq\bar{v}\rightarrow\mu_{b',b}^{\mathrm{up}}$$

$$\underline{v}\leq v_{b',b}^{\mathrm{dn}}\leq\bar{v}\rightarrow\mu_{b',b}^{\mathrm{dn}}.$$

[12] An intuitive explanation of the objective function is to consider lines buying at the bus b DLMP (when the flow is from b to b') and selling at the bus b' DLMP (when the flow is from b' to b).

It is worth noting that the deliverability of reserves, i.e., the actual offering of all the reserves promised when the contingency requiring their delivery in full occurs, is guaranteed through the imposition of the voltage magnitude constraints on $v^{up}_{b',b}$ and $v^{dn}_{b',b}$.

- Finally, the dual-variable-update step takes place at each bus b, after all subproblems associated with devices connected to bus b have solved. Note that each bus solves in parallel and asynchronously relative to other busses, since it can start solving as soon as all devices connected to it have solved. In fact, busses impose synchronization in a proximal sense. Each bus b uses the updated real and reactive power injection and voltage magnitude information corresponding to contingencies $y = 1(\text{up})$, $y = -1(\text{dn})$, and $y = 0$ (no superscript identifier) communicated by devices connected to it to perform the following three tasks.
  - Revise penalties $\rho^{P,k}_b$, $\rho^{Q,k}_b$, $\rho^{up,k}_b$, $\rho^{dn,k}_b$, $\rho^{R,k}_b$, $\forall b \in \beta^s$. $\rho^{P,k+1}_b = \text{func}\,(\rho^{P,k}_b,$ imbalances mismatches at primal subproblem iterations k and $k+1$) and similarly for $\rho^{Q,k+1}_b, \rho^{Q^{up},k+1}_b, \rho^{Q^{dn},k+1}_b, \rho^{R,k+1}_b$.
  - Update the DLMPs using the imbalances present in the device subproblem decisions during iteration $k+1$

$$\hat{\pi}^{P,k+1}_b = \hat{\pi}^{P,k}_b + \frac{\rho^{P,k}_b}{|A_b| + |H_b|} \times \left\{ \sum_{j \in A_b} P^{j,k+1}_b + \sum_{b' \in H_b} P^{k+1}_{b,b'} \right\}$$

$$\hat{\pi}^{R,k+1}_b = \hat{\pi}^{R,k}_b + \frac{\rho^{R,k}_b}{|A_b| + |H_b|} \times \left\{ \sum_{j \in A_b} R^{j,k+1}_b + \sum_{b' \in H_b} \frac{P^{up,k+1}_{b,b'} - P^{dn,k+1}_{b,b'}}{2} \right\}.$$

$$\hat{\pi}^{Q,k+1}_b = \hat{\pi}^{Q,k}_b + \frac{\rho^{Q,k}_b}{|A_b| + |H_b|} \times \left\{ \sum_{j \in A_b} Q^{j,k+1}_b + \sum_{b' \in H_b} Q^{k+1}_{b,b'} \right\}$$

$$\hat{\pi}^{Q^y,k+1}_b = \hat{\pi}^{Q^y,k}_b + \frac{\rho^{Q^y,k}_b}{|A_b| + |H_b|} \times \left\{ \sum_{j \in A_b} Q^{j,y,k+1}_b + \sum_{b' \in H_b} Q^{y,k+1}_{b,b'} \right\}, y = \text{up,dn}.$$

  - Convert line voltage magnitude constraint dual variables at line ends to the corresponding nodal values for use in convergence speed up filter [125] and update voltage magnitude discrepancy penalties at the ends of lines sharing the same bus:

$$\hat{\mu}^{k+1}_b = \sum_{b' \in H_b} \mu^{k+1}_{b,b'}$$

$$\hat{\mu}^{y,k+1}_b = \sum_{b' \in H_b} \mu^{y,k+1}_{b,b'}, y = \text{up, dn}$$

$$\hat{\varsigma}^{k+1}_{b,b''} = \hat{\varsigma}^{k}_{b,b''} + \rho^{v,k}_b \left(\frac{\sum_{b' \in H_b} v^{k+1}_{b,b'}}{|H_b|} - v^{k+1}_{b,b''} \right)$$

$$\hat{\varsigma}^{y,k+1}_{b,b''} = \hat{\varsigma}^{y,k}_{b,b''} + \rho^{v^y,k}_b \left(\frac{\sum_{b' \in H_b} v^{y,k+1}_{b,b'}}{|H_b|} - v^{y,k+1}_{b,b''} \right), y = \text{up, dn}.$$

1) Discussion of Distributed DLMP Algorithm: The first two of the three steps described above can take place in either order. Neither can commence, however, until after the third step of the previous iteration has completed and communicated a new set of DLMP estimates to all connected devices. The third step, which updates bus-specific DLMPs and voltage magnitude constraint dual variables, is in fact the one that implements a distributed synchronization mechanism. It waits for all connected devices to solve their subproblem and communicate their solution, even if it is unchanged from the previous one. It then updates DLMPs at that bus while all connected devices are idle. Once the updated bus-specific DLMPs are communicated to the connected devices, the device subproblems are authorized to solve again. Variations of this synchronization mechanism allowing bus DLMP updates to start before all connected device subproblems have solved are possible but do not appear to improve convergence.

Local convergence is observable at a bus when imbalances at that bus satisfy convergence tolerance criteria. Global convergence is achieved when local convergence is achieved simultaneously at all buses. Local convergence is communicated at the end of each bus iteration to proximal busses and eventually propagates to the substation root bus. Local convergence messages that reach the substation root bus from all downstream buses and persist over a number of iterations exceeding the depth of the longest distribution feeder is a global distribution network convergence certificate (see [5]). Thus, a global convergence certificate can be obtained through PMP as well, and does not require an information-communication-intensive coordinating super node.

Transmission LMPs that are compatible with DLMP scan be obtained with two alternative approaches.

— The centralized B, θ linearization can be decomposed to bus and line subproblems and a PMP distributed algorithm similar to the one described above, but limited to the discovery of LMPs $\pi^P_n(t)$ and $\pi^R_n(t)$, can be implemented.

— An efficient centralized shift factor algorithm can be solved repeatedly using as input the most recent available primal estimates from the various substation DLMP problem iteration $\hat{P}_{\infty_s,\infty_{s^*}}(t)$, $\hat{Q}_{\infty_s,\infty_{s^*}}(t), \hat{R}_{\infty_s,\infty_{s^*}}(t), \forall s \in N^S$. Under this second alternative, line ∞_s, ∞_{s^*} device DLMP subproblems will be allowed to resolve after they receive new DLMP estimates from bus ∞_{s^*} without conforming to the general requirement imposed on all other distribution feeder lines which stay idle until they receive a new DLMP at each of the two busses that they connect. When new $\hat{\pi}^P_{\infty_s}(t)$ and $\hat{\pi}^R_{\infty_s}(t)$ estimates are made available to line ∞_s, ∞_{s^*}, regularization terms must be designed carefully to avoid oscillations.

The preferred alternative will depend on T&D coordination issues and the extent to which DERs participate in the distribution market. Light DER participation will allow at first forecasting of $P_{\infty_s,\infty_{s^*}}(t), Q_{\infty_s,\infty_{s^*}}(t), R_{\infty_s,\infty_{s^*}}(t), \forall s \in N^S$quantities that are as accurate as we are able to obtain today. This implies that the behavior of DERs will most likely have a minor influence on LMPs, allowing DLMP pricing to a few pioneering distribution market participants to be implemented with an initially simpler, forecast-based, T&D coordination. Fully integrated T&D LMP discovery will then have the opportunity to be adopted in a stage-wise manner.

B. Distributed Architecture: Computation-Communication Requirements and Convergence

To analyze the computation and communication requirements of the distributed architecture described above we define the following computation/optimization and communication tasks.

1) As noted above, each single-bus and two-bus connected device subproblem solves in parallel conditional upon tentative marginal-cost-based prices at that bus. Solutions of tentative $P, Q, Q^{\text{up}}, Q^{\text{dn}}, R, v$ values are communicated to the proximal bus(es). We assume that the slowest device subproblem solves in time τ_1. T&D interface buses ∞_s communicate distribution network reserve provision $R_{\infty_s,\infty_{s^*}}(t)$ to the zonal reserve requirements coordination bus.
2) Each bus updates T&DLMPs and voltage constraint dual variables so as to decrease imbalances, and communicates them to each device (line or DER) connected to that bus. Each zonal superbus communicates the updated reserve clearing price to each transmission bus in the zone. We assume that the slowest bus update takes time τ_2.
3) At Δk iteration intervals, the voltage dual variable estimation correction filter and its feedback to T&DLMP corrections (see [125]) is executed involving $|\beta s|$ buses for each $\infty_s \in N^S$. Each bus communicates $P, Q, Q^{\text{up}}, Q^{\text{dn}}, R, v$ information, i.e., six numbers, to the filter-executing superbus and receives an equal number of tentative prices back. We assume that the slowest substation filter execution takes time τ_3.
4) At each iteration, local convergence is defined at each bus as the resolution of imbalances. Global convergence verification requires the assurance that all buses $|N^T| + |N^S||\beta s|$ have converged. This requires an additional coordinating bus that identifies convergence by communicating with each transmission n and substation bus $b \in \beta_s \forall s \in N^S$. For substation buses, the tree structure of distribution feeders can be used to propagate convergence certification to the substation feeder root bus with negligible communication delay [5]. Since global convergence verification can occur independently of the iterative solution process, the associated communication delay may at worst require a few superfluous iterations before global convergence is actually verified.

Regarding computation and communication requirements described in Table 2, we note the following.

Experience—albeit simulation based and not really extensive—[1], [2], [5], [13], [125] has reinforced the expectation that the algorithm's distributed and naturally parallelizable nature is insensitive to problem size. Indeed, numerical experience on a single period market discovering only real power T&DLMPs and involving ~1 million decision variables requires in the order of thousands of iterations to converge [1]. Solving multiperiod day-ahead markets with real and reactive power DLMPs and DERs with intertemporally coupled dynamics has provided evidence that the number of iterations needed to converge is also weakly—in fact sublinearly—related to problem size [5] represented by the network's number of buses $|N| + |\beta_s||N^S|$, or perhaps more accurately its depth. Typical T&D network topologies exhibit $|N| \sim$ 3–10 thousand, $|N^z| \sim$100–500, $|\beta_s| \sim$1000–50 000, $|\text{Ab}| =$ 1–30, and $|\text{Hb}| =$ 2–5.

Given the parallel, distributed (and potentially asynchronous so as to avoid the burden of a synchronizing time signal) solution of individual subproblems, the communication of each subproblem solution to the nearest bus(es) is relevant only for the slowest subproblem at each bus which communicates to and receives from the imbalance processing bus only a handful of numbers. Hence, the communication delay per iteration is of the order of milliseconds. Cyberattacks and malicious data manipulations in the optimization loop are nevertheless an issue. This is discussed in Section IV.

Task iii) is the most demanding, both computationwise and communicationwise. If we opt for a centralized transmission dc approximation-based LMP iteration, the associated computation burden will be significant as well. In both cases, however, these high resource consuming

Table 2 Communication and Computation Requirements for K Iterations to Convergence

Task	Computation time upper bound	Computation time for K iterations to convergence	Data Communications (P,Q,Q^{up},Q^{dn},R,v), (T&DLMPs and μ) per iteration per bus	Data to/from Coordinating Bus per iteration per Coordinating Bus
i	τ_1	$K\tau_1$	$6\max_b A_b$	$\lvert N^z \rvert$
ii	τ_2	$K\tau_2$	$6\max_b A_b$	$\lvert N^z \rvert$
iii	τ_3	$K\tau_3/\Delta k$		$12\max_s \lvert\beta_s\rvert$
iv			6	$\lvert H_b \rvert$
Total		$K(\tau_1+\tau_2+\tau_3/\Delta k)$ or since task *iii* occurs in parallel, $K(\tau_1+\tau_2)$	$6+12\max_b \lvert A_b \rvert$	$2\lvert N^z \rvert+12\max_s \lvert\beta_s\rvert+\lvert H_b \rvert$

tasks will not be executed as often as bus- and device-specific subproblems. In fact, they will be executed once in every Δk nodal subproblem iterations without requiring that meanwhile the subproblems remain idle.

We finally note that distributed solution of subproblems, given offline calibration of expected intrahour t reserve deployment cost $\bar{J}(R_b^j(t))$, and asynchronous, coordinating bus problem solutions require $(\tau 1+\tau 2)\sim$ milliseconds.

The tractable computation and communication requirements discussed above suggest the proposed distributed architecture is applicable to real T&D systems. However, although tractable convergence proof of concept is in hand [1], potential improvements under asynchronous subproblem solution iterations, distributed penalty adaptation, and convergence certification via nearest neighbor information dissemination of local convergence observations [5], [125] require further work. In addition, nonconvex ac load flow problems can be adequately convexified for radial nonmeshed systems building on work by Low *et al.* [27], [28], [50], reverse flow can be addressed [5], and ac feasible T&DLMPs can be obtained by relying on adaptive linearization gap linear transmission network load flow that captures losses and ac feasibility [14].

Finally, nonconvex subproblems, arising among others with generator marginal costs that are not monotonically increasing, do not satisfy strong duality requirements resulting in the proposed price-directed decomposition's inability to achieve any generation level that may be primal optimal. They work well, however, if the primal optimal solution is in the higher capacity utilization range where the total cost is locally convex. We have observed and proven the existence of noncompetitive equilibria in coupled energy and reserve markets under large coalitions of load or DER aggregations [3]. As discussed further in Section IV, empirical observations indicate that such conditions are relevant and can likely motivate acceptable regulatory solutions.

We consider a detailed discussion of the specific communication medium that may be selected to implement the distributed architecture sketched above to exceed the scope of this paper. Whether it will be based on PLC, WiFi, cable or wireless Internet, or a mix utilizing interface standards, it will likely rely on a platform that allows DERs to be certified in a streamlined manner and to participate in the market at will, provides decision support and the like.

IV. T&DLMP CLEARING MARKETS: COMMENTARY ON CYBERSECURITY, TOPOLOGY CONTROL, AND MARKET DESIGN IMPLICATIONS

A. Distributed Computation and Communication T&DLMP Clearing Architecture Is Compatible With Cybersecurity Remedies

The proposed distributed T&DLMP discovery architecture enables the design of cyberattack detection and avoidance protocols that capitalize on its PMP nature. Focusing on cyberattack scenarios where the data communication driving our PMP architecture plays a vital role [150], we note the following.

Intrusions to bus computations, also known as Byzantine attacks, can be detected quickly by exploiting the distributed nature of PMP, and the attacked buses can be deactivated in time to carry on the computation with the remaining healthy buses. Supervisory controllers that detect "which" control or estimator bus has been compromised can be designed using selective sampling strategies such as round robbin [151], push sum [152] and probing. The supervisory bus may run these detection algorithms in parallel without hindering normal operation. As mentioned already, once the malicious buses or sources of data are identified they can be isolated so that the controllers that enable the healthy part of the communication system may continue to function. Overall convergence times may suffer, however, due to the interruptions caused by the bus isolation process, depending on how many times an attacker intrudes into the system and corrupts any data source.

Intrusions to communication links that reflect themselves as denial-of-service attacks (or more specifically, a maliciously manipulated delay) can be prevented by employing adaptive controllers that protect the stability and convergence of microgrid protocols. Recent work [74] on arbitration-based optimal control designs also exploits delay-aware controllers. These preliminary results can be extended using ideas of sensor redundancy drawing from work by Marzullo [75], De Persis and Tesi [76], and Chakrabortty [71].

Attacks in the physical layer are also possible, say for example in the form of manipulation of setpoints to the transformers, DERs, storage, and loads. Three preliminary and yet seminal studies recently reported in [153] show that the complex, nonlinear (and, in many cases, nonsmooth) dynamic models of new power electronic converters such as the SST, if regulated with incorrect setpoints, may pose serious limits on the line currents and voltages in a distribution system beyond which its model experiences a Hopf bifurcation leading to sudden vanishing of feasible equilibria. When the operating conditions are manipulated by a hacker in a smart and coordinated fashion, the system equilibrium may be located right at the boundary of the infeasibility and Hopf bifurcation zones, or of the stability and subcritical bifurcation zones in the phase plane of the SST model. If the power signals coming from these intermittent DER sources vary over time, so will the system equilibrium. Depending on the severity of the setpoint manipulation in the attack space, the model parameters then may even migrate to unstable or infeasible zones. Linear output feedback controllers guaranteeing only load-generation regulation will obviously no longer be sufficient in such a scenario. Advanced detection algorithms that can quantify the trustworthiness of setpoint commands for these converters, followed by design of nonlinear controllers that can track and stabilize all feasible equilibria, will be needed instead. One would then derive intrusion detection algorithms that can quantify trustworthiness of setpoints by explicitly exploiting the mathematical relationship between the equilibrium of the rectifier, gyrator, and inverter stages of an SST and the injection level of 1) generation from renewables such as wind and solar PV (connected via both ac and dc links); 2) storage from battery; and 3) demand from the loads. The algorithm must continuously compute the operating limits of these sources and sinks to detect any setpoint command that fails to maintain the trajectory in the stable regions of the equilibrium space. One may also design nonlinear controllers that stabilize the derived family of equilibrium trajectories in situations when a given setpoint command cannot be fully trusted.

Our distributed architecture allows planning ahead for resilient cyber–physical architectures. Information-theoretic algorithms can be developed to determine in real time or on the fly which subproblem's primal variable estimates have the highest relative share in determining the nodal balance estimates. Thus, even if a certain number of links are unavailable due to an attack, one can always plan to reroute those preselected "important" subproblem solution outputs to be accounted for in the balancing and DLMP price update function of an available neighboring bus, and preserve the overall DLMP estimation accuracy. This effort is synergistic to the periodic execution of the accuracy-improving filter discussed in Section II-B2d. Prior expectations across buses can be tightened with Bayesian updates by employing information-theoretic metrics such as "mutual information" between different controllers and computing buses in the PMP algorithm to continuously keep track of the identity of the most influential estimators. In the event of expected or suspected attacks, the important links can be secured with tighter security measures.

B. Distributed Architecture and Topology Control in Feeder Networks: Operational Efficiency and Smart Islanding

1) Operational Efficiency: In the day-ahead T&DLMP implementation of the proposed distributed CPS architecture, hourly varying discrete decisions on centralized generation unit commitment and T&D network topology may provide significant economic benefits by mitigating line flow and voltage constraint congestion, decreasing distribution losses and enhancing reserve deliverability at distribution feeders. Extensive work on optimal topology control in transmission networks [14], [45], [47] has documented the advantages of relying on LMP-based sensitivities to drive desirable transmission network topology changes. Relying on DLMPs to identify hourly distribution network topology changes adds another hierarchical layer for short-term distribution network planning, in fact, integrating it to transmission planning.

2) Smart Islanding Under Emergency Conditions and Associated Stability Concerns: Under islanding conditions, the performance layer of our distributed T&DLMP architecture can offer an organic way to elicit load side response and reserve offering that is compatible with the islanded microgrid requirements. The interaction of cells $P_{4,2}$ and $P_{5,2}$ with cells $C_{5,2}$ and $C_{6,2}$ shown in Table 1 describes the crucial cyber and physical system interfaces that become relevant under these circumstances. We address below physical system pre-islanding contingency planning and post-islanding control that constitute the requisite CPS interface.

3) Contingency Analysis Through Critical Cut Set Discovery: In contrast to *ad hoc* islanding implementations used today in the event of severe damage by natural calamities, it is possible to employ max-flow min-cut graph concepts in order to develop a systematic and better-informed framework for pre-islanding contingency planning. The objective is to characterize the "brittleness" of the power

network by discovering the weak link(s) in the network graph through which disturbance modes can propagate relatively easier, depending on the link topological features, their reactances, the presence of strong control devices such as SVCs, SSTs, dominant loads, etc. In some cases, the flow through a link may not carry much information about the disturbance signatures at the points of origin of a large load (due to damping, high inertial factors of the load, etc.). Hence, it may be beneficial to construct an index indicating the strength of a path. Indeed, the recent work in [68] and [69] based on steady-state power imbalances has been extended to focus on the strength of the network in transience by using the energy function of the predisturbance grid model [70]. Online PMU measurements can be used to continuously update the energy function, compare combinations of energy transfers, and choose the weakest link.

4) Guarantee of Post-Islanding Performance: Stability and performance guarantees of the healthy part of the grid after it gets islanded from the damaged part can be guaranteed by replacing current *ad hoc* approaches with the design of fast-acting adaptive controllers that learn about the system conditions from online PMU measurements, and retain internal stability and robust performance of the power flows. Bump less transfer of control is very much desired in these situations to avoid very large current transients. Wide area feedback can be used to discover the minimal set of PMU measurements to be fed back to appropriate controllers so as to protect the closed-loop system from running out of synchronization and creating such dangerous transients, while at the same time avoiding undesirable overcommunication. Since in emergency situations the exact model of the healthy grid is unknown, PMU data can enable its identification in real-time using. The recent results on identifiability of graphs using Markov parameters as well as other related works on network identification [71]–[75] provides a significant step in this direction.

C. Distributed Computation and Communication T&DLMP Clearing Architecture: Individual Choice and Market Performance

The proposed distributed architecture enables a market design that enables individual market participants to make bids/offers of coupled product and services (real and reactive energy and reserves) that are consistent with their preferences and a wealth of relevant but only locally available information (weather, dynamic preferences, physical constraints, and degrees of freedom). Our distributed architecture leverages the increasingly affordable advanced metering and decision support information technology for full ex-post cost accountability. More specifically, it enables the implementation of market participation rules that do not motivate market gaming and foster the discovery of stable clearing prices. Despite distributed, local optimization and balancing decisions, proximal-message-passing-based price propagation is sufficient to reach global convergence to a stable market equilibrium. The following discussion addresses these equilibrium properties and additional actions that may be required to achieve an efficient system balance.

As is known, for the wholesale market, there are conditions with nonconvex problems where additional "uplift" payments are required to complement the efficient commitment and dispatch solution [118], [121]. A similar logic applies to the analysis of DLMP and the distribution market. Given the existence of a market price equilibrium, our PMP approach provides highly attractive properties for finding solution in a highly parallel structure with decentralized information.

In the cases where an equilibrium price vector does not exist, the logic of extended locational marginal pricing in wholesale markets should be adapted to the particular conditions of distribution markets. The goal is to establish market equilibrium and associated pricing conditions that can achieve the efficient outcome of economic dispatch. In the first instance, market clearing design should focus on the structure of algorithms and pricing that support this efficient outcome under the assumption that market participants act as price takers. This is the competitive market ideal. Without this necessary minimal design structure, efficiency is unlikely. Given this workably efficient design, the next step is to consider the opportunities for identifying and addressing strategic behavior in exploiting market power. In the wholesale market, for example, it is well known that conditions can exist—notably under transmission congestion—that give rise to generator market power. It is also well known that these conditions are relatively rare and can usually be dealt with through the application of straightforward "offer-cap" rules that maintain the efficient competitive outcome [120]. Two examples of distribution market malfunction are noted.

1) Reactive power: Our work on realistic distribution networks indicates that volt/var control devices, such as power electronic instantiations of ubiquitous inverters, may be exposed in a non-gold plated, i.e., nonoverbuilt, distribution network to situations that allow them to exercise market power by capacity withholding. Congestion in distribution networks occurs when voltage levels in some locations reach their upper or lower acceptable limit. Under congestion conditions, volt/var control devices may be able to withhold, say, 10% of their capacity to cause a much higher percentage increase in the price of reactive power. Of course, such incidences are more likely under energy-service-company-type service aggregation conditions.
2) Reserve deliverability: Another likely troublesome market malfunction arises when the distribution network's voltage magnitude limitations prevent the deliverability of the reserves market

participants are willing to offer. To deal with these CPS interactions, we have proposed a market rule in Section II-B2d that translates the contingency of possible voltage magnitude limitations during a future reserve deployment request to a Lagrange multiplier that affects the reserve DLMP.

Following empirical study of the likely severity of incidences that are nonaddressable by economic efficiency rationality, practical and economically efficient regulation should be considered that blunts market power or physical-system-wise unenforceable situations.

Research on the extensions of wholesale power markets to retail/distribution networks must focus on identifying the conditions where market power could arise and seek policies that promote efficient post-market-offer-cap outcomes.

An important development in wholesale power markets has been the expansion of market design to consider operating capacity scarcity, co-optimization of energy and reserves, and the associated integrated pricing [117], [119]. These operating reserve models focus on real power to meet short-term deviations in real power supply balance. Although a similar treatment of reserves might be applicable to the distribution system, given the importance of voltage constraints and reactive power requirements on the distribution system, wholesale models must be extended to include both real and reactive power management.

We close by noting that our distributed T&DLMP discovery architecture is already considering the availability and response characteristics of reserves, co-optimization in the dispatch, deliverability limits on the distribution feeders, and the implications on energy, reactive power and reserve pricing.

V. INDIVIDUAL DER SUBPROBLEMS AND THEIR CYBER–PHYSICAL INTERFACES

As noted in Section II, distributed DER subproblem optimization rests on cyber/market clearing layer model of its dynamics and bidding costs and capabilities. This requires 1) reduced model of the underlying real time physical system dynamics and 2) offline cost studies of reserve deployment contingencies yielding expected intrahour t reserve deployment cost $\bar{J}(R_b^j(t))$ and the associated optimal reserve deployment response policies that the DER will actually rely upon during actual deployment requests. Both requirements rely on a thorough understanding of the DER physical models. In this section, we comment briefly on selected DERs including battery storage/EV battery charging, heat pumps with or without combined heat and power (CHP) microgenerators, data centers, and volt/var control devices.

A. EV Charging in the Multiperiod Day-Ahead Market and the Physical Battery Model

The physical EV battery system's charging capabilities are sensitive to nonlinear electrochemistry dynamics that depend crucially on the history of charging discharging actions. We all know, for example, that a 50% charge of a Tesla's battery takes a coffee break whereas the remaining 50% requires a long lunch break. Moreover, we know that the life of a battery depends on the number and profile of past charge discharge cycles. It is therefore important for EV DERs to schedule real power, reactive power, and reserve bids/offers using a realistic cyber/performance layer subproblem at the market time scale, and similarly to respond to real-time reserve deployment requests using an accurate time-differential-equation physical model of the EV battery. We note again, that, whereas ideal battery model approximations adopted for computational tractability by proposed centralized market clearing algorithms [3], [5] limit decision efficiency and implement ability, our distributed architecture enables the use of accurate models.

It is important to understand that efficient EV charging decision support for full DLMP market participation remains to be developed. It requires understanding the battery conditions and how charging/discharging will affect the battery voltage over both short and longer time scales impacting both the instantaneous capacity to charge as well as long-term battery life. To this end, detailed electrochemical physical system models of typical Li-ion batteries must be developed in order to enable model reductions that connect the detailed physical model to the EV battery-charging subproblem. Reduced cyber models must be strategically selected to be computationally less expensive than the physical model while capturing the salient characteristics that the distributed architecture can handle. Offline solutions of the differential-equation-based physical battery model should be applied to the development of real-time ISO reserve deployment response policies and associated expected intrahour t reserve deployment cost functions $\bar{J}_t(R(t))$. Published work by Ryan [111]–[114] and others [109], [110], including related work applied to carbon capture technologies [115], [116] is relevant to such future research efforts. An illustrative reduced CPS architecture EV DER subproblem is given below after omitting bus location and regularization terms. Denoting the state of charge (SoC) at time t, by $X(t)$, modeling charging capacity $C(X(t), R(t-1), P(t-1))$ as a function that depends on the current SoC and past reserves and charging decisions, the value to the EV owner of the SoC at the departure time T, by $U(X(T))$, real and reactive power consumed at t, by $P(t)$and $Q(t)$, and regulation service reserves offered during period $[t, t+1]$, by $R(t)$, we have

$$\max_{P(t).Q(t),S(t)} \left\{ \sum_{y=t_0}^{T-1} \left[\pi^Q(t)Q(t) + \pi^R(t)R(t) - \pi^P(t)P(t).. \right. \right.$$
$$\left. \left. + U(X(t)) + \bar{J}_t(R(t)) \right] \right\}$$

$$\text{s.t.} \quad X(t+1) = X(t) + P(t)$$

$$P(t) \le C(X(t), R(t-1), P(t-1))$$

$$(Q(t))^2 \le C(X(t), R(t-1), P(t-1))^2 - P(t)^2$$

$$R(t) \le \min\left\{ (P(t); \sqrt{C(X(t), R(t-1), P(t-1))^2 - Q(t)^2} - P(t) \right\}$$

where $\bar{J}_t(r)$ represents the expected intrahour t reserve deployment cost associated with the promised reserves R. In the above, we do not consider for simplicity Q^{up} and Q^{dn} decisions.

Note again that the market participation cyber model will operate at a market appropriate time scale which is of the order of five minutes or longer, while the physical model that is capable to estimate $\bar{J}_t(R(t))$ should be able to discriminate time at the four second regulation service time scale, and as such, rely on approximate DP approaches of the type employed among others in [4], [11], [15], [18], and [22].

B. HVAC: Heat Pump-CHP Micro Generator Collaboration Example and Generalization

We consider an illustrative simple model of a CHP microgenerator powering a heat pump-based HVAC system. We omit location designation and regularization terms and use the following definitions.

State:

— $X(t)$: Temperature at the end of hour t inside a building, subject to boundary condition $X(24) = X(0)$.

Decisions:

— $P^h(t), Q^h(t), R^h(t)$ in KWh, KVarh, KW representing the real power, reactive power, and secondary reserve decisions associated with the heat pump that are effective during each hour $t = 1, 2, \ldots, 24$, and boundary condition $X(0)$ which is decided by the "storage-like" DER.

— $P^{mg}(t), Q^{mg}(t), R^{mg}(t)$ in KWh, KVarh, KW representing the real power, reactive power, and secondary reserve decisions associated with the microgenerator that are effective during each hour $t = 1, 2, \ldots, 24$;

— $H^{mg}(t)$: KWh of heat (or cool) provided to the building through full or partial waste heat recovery from CHP microgenerator.

Inputs:

— α^{mg}: Variable cost per kWh of electricity generated by microgenerator;

— c^h: increase in inside degrees/kWh consumed by heat pump;

— c^{mg}: increase in inside degrees Celcius/kWh of microgenerator waste heat utilization;

— L^h: heat loss coefficient representing the decrease in degrees Celcius occurring per degree hour difference inside and outside temperature;

— η^{mg}: kWh of heat (or cool) recoverable per kWh of electricity generated by the microgenerator;

— $T^{outside}(t), t = 1, 2, 3, \ldots, 24$, outside temperature trajectory during each hour t;

— $\underline{T}_b(t), \bar{T}_b(t), t = 1, 2, \ldots, 24$, inside temperature comfort bands;

— $\bar{P}^h$, $\bar{P}^{mg}$: capacities of heap pump consumption and microgenerator electricity output.

The resulting subproblem is

$$\min_{X^h(0), P^h(t), Q^h(t), R^h(t), P^{mg}(t), Q^{mg}(t), R^{mg}(t), H^{mg}(t) \forall t = 1,2,\ldots,24}$$

$$\sum_{t=1,24} \left[\pi^P(t) P^h(t) - \pi^Q(t) Q^h(t) - \pi^R(t) R^h(t) \right]$$

$$- \sum_{t=1,24} \left[\pi^P(t) P^{mg}(t) + \pi^Q(t) Q^{mg}(t) + \pi^R(t) R^{mg}(t) \right]$$

$$+ \sum_{t=1,24} \left[\alpha^{mg} P^{mg}(t) + \bar{J}^h\left(R^h(t)\right) + \bar{J}^{mg}(R^{mg}(t)) \right]$$

subject to

$$X^h(t) = X^h(t-1) + c^h P^h + c^{mg} H^{mg}(t) - L^h \left[\frac{X^h(t) - X^h(t-1)}{2} - T^{outside}(t) \right]$$

$$\forall t = 1, 2, \ldots, 24$$

$$0 \le P^h(t) \le \bar{P}^h, \qquad \text{for all } t = 1, 2, \ldots, 24$$

$$0 \le R^h(t) \le \min\left\{ \bar{P}^h - P^h(t), P^h(t) \right\}$$

$$\forall t = 1, 2, \ldots, 24$$

$$- \sqrt{(\bar{P}^h)^2 - \left(P^h(t) + R^h(t)\right)^2} \le Q^h(t)$$

$$Q^h(t) \le \sqrt{(\bar{P}^h)^2 - \left(P^h(t) + R^h(t)\right)^2}$$

$$0 \le P^{mg}(t) \le \bar{P}^{mg}, \qquad \text{for all } t = 1, 2, \ldots, 24$$

$$0 \le R^{mg}(t) \le \min\left\{ \bar{P}^{mg} - P^{mg}(t), P^{mg}(t) \right\}$$

$$- \sqrt{(\bar{P}^{mg})^2 - \left(P^{mg}(t) + R^{mg}(t)\right)^2} \le Q^{mg}(t)$$

$$Q^{mg}(t) \le \sqrt{(\bar{P}^{mg})^2 - \left(P^{mg}(t) + R^{mg}(t)\right)^2}$$

$$0 \le H^{mg}(t) \le \eta^{mg} P^{mg}(t)$$

$$\underline{T}(t) \le X^h(t) \le \bar{T}(t)$$

whereas the above model is stylized and simplified, it illustrates that the proposed distributed architecture allows modeling of the real-time hybrid (discrete and continuous state variable) dynamic behavior of HVAC

systems and their market time-scale equivalent. The physical HVAC system can be adequately represented by complex constrained optimization models which are compatible with our distributed CPS architecture. Indeed, a key advantage of our distributed CPS architecture is the simultaneous discovery of tentative HVAC decisions and T&DLMPs, enabling model-predictive control to identify the schedule of HVAC operation on a day-ahead basis as a function of dynamic DLMPs [101]. Research to date [102]–[105] shows the efficacy of obtaining substantial benefits when the day-ahead DLMPs are known, with the benefits increasing further and the HVAC's operation becoming less "nervous" when reserves are also co-optimized. In short, unlike a generator, a building has storage capacity, and limits on power flow that are conceptually similar to other storage devices but with slower dynamics and higher electromechanical complexity. Preliminary work by Baillieul *et al.* [80] shows indoor temperature (constrained within comfort limits) and electrical power for a base case and two cases of reserve response. Extensions to more realistic (i.e., multizone) buildings and DLMP-based optimization as well as effective physical system modeling that interfaces building-level optimization with device-level (i.e., chiller) control are necessary new research directions. In principle, the latter should be straightforward: the variable speed drive associated with the induction motor for the chiller (or the speed control for a dc motor) is adjusted directly to produce the desired demand for electrical power, through a feedback controller that incorporates proportional, integral, and derivative gains based on empirical tests or chiller dynamic models. In practice, however, direct control of chiller speed may be impractical, because chiller manufacturers incorporate proprietary control sequences that limit the range of frequency adjustment in order to prevent problems associated with vapor compression machinery. Until such time as chiller manufacturers make their units "grid friendly," which we hope will materialize in the not too distant future, a feasible approach might be to control the chilled-water setpoint, the typical input to current chiller controllers.

C. Data Centers

Computing as exemplified by data center server farms is possibly one of the most versatile DERs. Past work on data center power management has been extended by recent work on data-center-provided fast reserves [18], [19] to fully translate physical power system behavior to power market time-scale subproblem development. In particular, given the diversity of data center power consumption response capabilities ranging from microseconds (DVFS) to 1–30 s (server sleep/readiness state control) to 5–30 min (cooling), data centers are capable of providing a wide selection of reserves and participate in power markets for great mutual benefit. Encouraging results on real-time physical data center modeling show that approximate stochastic DP [18] can provide excellent regulation reserve service deployment that trades off optimally among timely computing job completion quality of service and regulation signal tracking. Homogeneous-computing-load results must be extended to multiple-job-type situations. Efficient data center market bidding and real-time response to reserve deployment require further decision and control achievements. Approximate stochastic DP policies promise to render data center reserve provision implementation ready.

D. DERs With Distributed Volt/Var Control Devices

Devices providing distributed and dynamic volt/var control are expected to be widely available and connected to multiple distribution network locations in the very near future. For example, "smart" PV inverter–converter power electronics contain a capacitor capable of providing not only the inertia missing from nonrotating generators but also a dc bus enabling the wirelessly communicating inverter to provide flexible and price responsive reactive power compensation even after sunset. EV battery chargers and other smart appliances accompanying power electronics have similar capabilities that can be harnessed for volt/var control given the requisite information communication. Recent and upcoming changes in standards will only reinforce this trend. On December 22, 2014, California's Public Utilities Commission (PUC) issued Decision 14-12-035, adopting modifications to California's Electric Tariff Rule 21, intended to leverage the capabilities offered by smart inverter technology. The modified rule requires all new distributed generation interconnecting via PUC's Rule 21 process to have a smart inverter in the near future. In a similar vein, IEEE1547a amendment was adopted in 2014 paving the road for the deployment of smart inverters by relaxing many restrictions imposed by the original IEEE 1547 standard. These devices are in the process of being deployed at Southern Company. Other products entering the market include SST technology currently investigated and developed by the Future Renewable Electric Energy Delivery and Management Systems Center (FREEDM Center) at the North Carolina State University (NCSU, Raleigh, NC, USA) [7], power electronics solutions by Gridco systems, distributed solutions by Varentec, etc.

However, concerns have been voiced that a large-scale deployment may harm distribution systems or that they may not perform as advertised with potential problems including: 1) robust operation of these devices during poor power quality; 2) incompatibility of smart inverters from different manufacturers; and 3) unwanted control interaction between autonomously acting inverters. Furthermore, choosing the right voltage control strategy for smart inverters is crucial in order to ensure efficient voltage control in the presence of solar output variability. Implementation of the proposed distributed

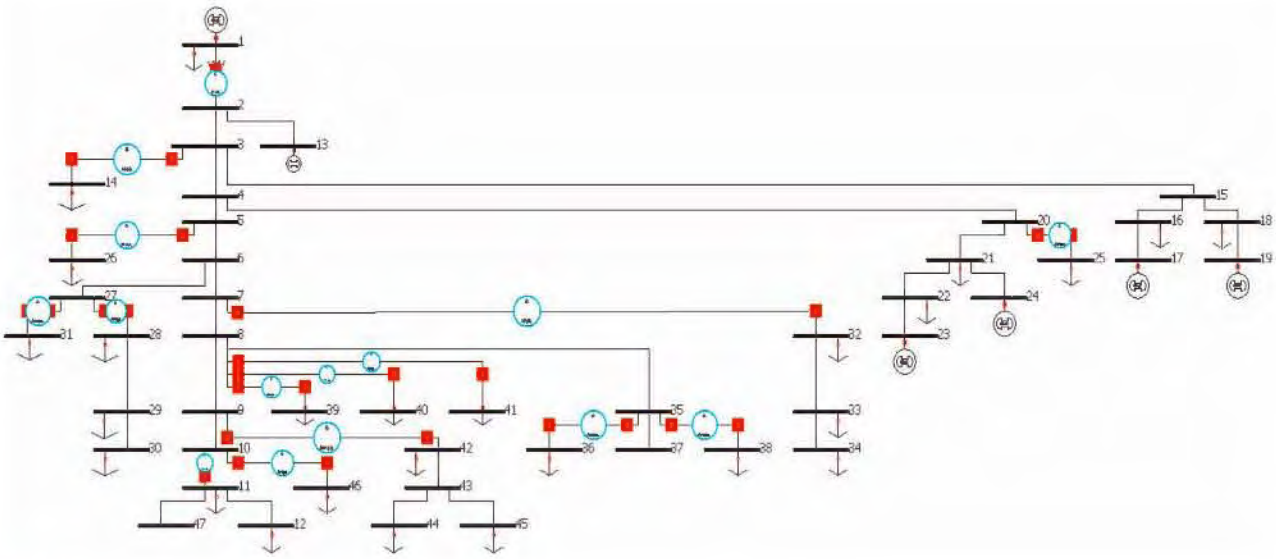

Fig. 5. *The 47 bus network topology diagram showing lines, transformers, and load busses.*

T&DLMP discovery architecture must be preceded by thorough investigation of tho aforementioned concerns on two fronts: 1) detailed field studies of tho impact of DLMP-driven distributed volt/var control devices on load flow characteristics (including harmonics and other related quality characteristics) measured through the deployment of accurate real-time monitoring sensors; and 2) careful computer simulation (see, for example, [16]) that can duplicate the actual measurements and thus gain the requisite credibility for performing analyses that precede and clear the way to actual implementation.

VI. NUMERICAL RESULTS

We provide some illustrative numerical results of a distribution market with active distributed participants who participate in the clearing of DLMPs in a 24-h day-ahead market setting. The market clearing problem was solved using the advanced integrated multidimensional modeling software (AIMMS) modeling framework that provided unique optimal primal and dual solutions as guaranteed by the radial network topology of the network that we used.

In particular, we report results obtained primarily on a 47-bus test feeder based on the network described in [27] and used extensively in numerical studies by Low and others. To the network reported in [27] we added primary to secondary voltage transformers at load busses and a subtransmission to primary voltage transformer at the substation. We modeled a significant portion of the load as inflexible nonresponsive commercial low-voltage demand, increased the resistance and reactance of distribution lines by a factor of 1.5, introduced some flexible electric vehicle battery charging demand, and replaced the PV in [27] with distributed microgenerators. The inflexible loads were modeled with the same peak as in [27] and a reactive power consumption power factor of 0.8. The 47-bus network topology is shown in Fig. 5 with additional input data reported in the Appendix. Some interesting results obtained from a realistic 800-bus distribution feeder documented in [149] are also reported to provide a real life perspective.

Figs. 6–8 show the maximum and minimum hourly DLMP trajectories for real power, regulation reserves, and reactive power. We do not report the reactive power DLMPs under the +1 or −1 regulation signal contingencies, but note that they turn out much smaller in magnitude, i.e., $\pi_b^Q(t) \gg \pi_b^{Q,\mathrm{dn}}(t)$ and $\pi_b^Q(t) \gg \pi_b^{Q,\mathrm{up}}(t)$.

It is interesting to note the following.

1) DLMPs vary across the distribution feeder's busses, as indicated by the spread between the maximum and minimum values during the same hour. This spread increases for distribution network that contain distribution feeders that serve different

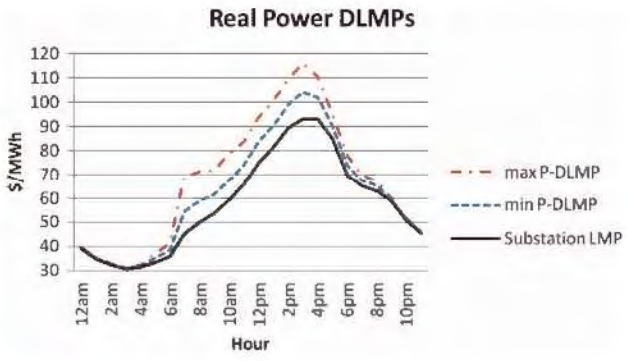

Fig. 6. *Minimum, maximum, and substation real power DLMPs.*

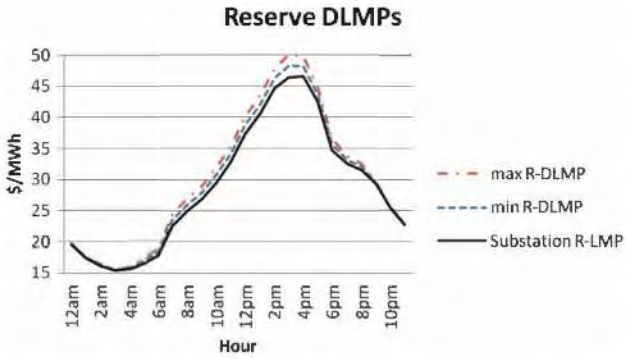

Fig. 7. *Minimum, maximum, and substation reserve DLMPs.*

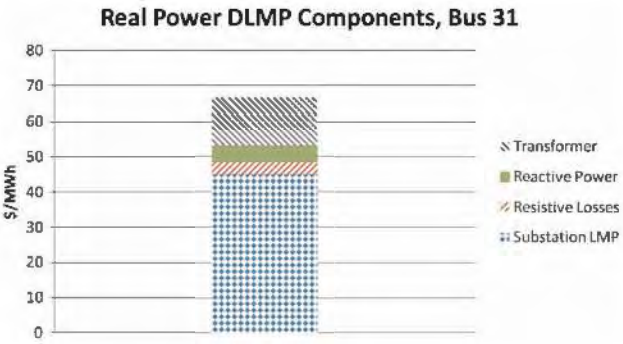

Fig. 9. *Real power DLMP decomposition (bus 31, system peak hour).*

consumers, as, for example, feeders with a widely different residential/commercial mix, and hence weekly correlated feeder load profiles. An example where this is the case is exemplified in Fig. 14 that reports real power DLMPs from a more diverse 800 bus distribution feeder with residential and commercial feeders where load profiles peak at different times. In that case, the locational incentives for distributed generation such as PV solar are even stronger than those exhibited in the 47-bus feeder DLMP spread.

2) DLMPs are in most cases higher than the substation bus LMP during each of the 24 h. Although this is a recurring pattern, due, among others, to the fact that line losses require the power flowing into the substation to exceed the power consumed at distant feeder buses, there are several DLMP observations that are smaller than LMPs. The reserve DLMPs $\pi_b^R(t)$ become smaller than the reserve LMP, during hours that a distribution feeder becomes a net exporter, as is the case for late night hours in the large DG capacity scenario reported in Fig. 13. Smaller DLMPs than LMPs are also encountered with real and reactive power DLMPs. For example, when PV generation is high relative to load at a bus close to the substation, real power DLMP at that PV bus may dip to reflect binding upper voltage magnitude constraints and reactive power DLMP may not only decrease but may also become negative. The combination of lower real power DLMPs and negative reactive power DLMPs makes it more profitable for the PV to inject less real power, using the freed capacity to consume reactive power in order to alleviate the voltage constraint. The locational incentives of the optimal DLMPs are thus clear.

Figs. 9–11 present the various building blocks of real power, reserve, and reactive power DLMPs, respectively, for the feeder peak load hour and for bus 31, which is located relatively far from the distribution substation.

Note that the substation LMP (the opportunity cost at the substation in the case of the reactive DLMP) is dominant. Nevertheless, transformer life loss costs are also significant. In the case of the reserve DLMP, we see an almost perfectly symmetric contribution of reserves up and reserves down. If up and down regulation were to be split into different reserve products, or if the

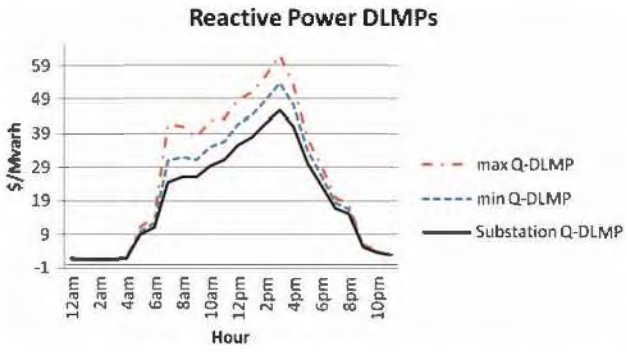

Fig. 8. *Minimum, maximum, and substation reactive power DLMPs (for regulation signal zero).*

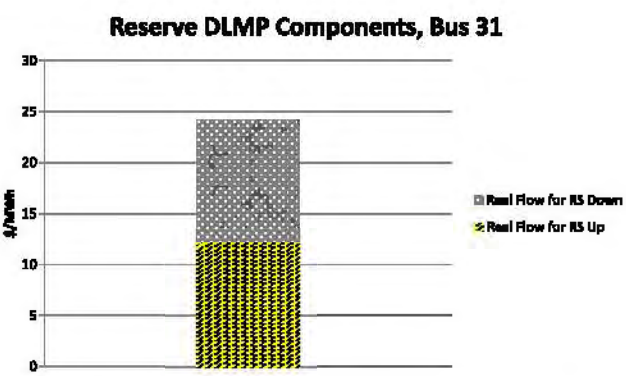

Fig. 10. *Reserve DLMP decomposition (bus 31, system peak hour).*

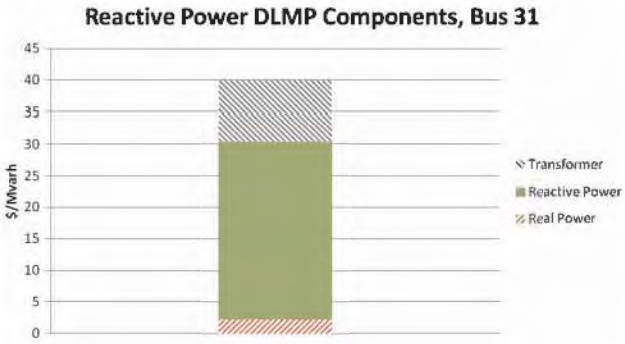

Fig. 11. *Reactive power DLMP decomposition (bus 31, system peak hour).*

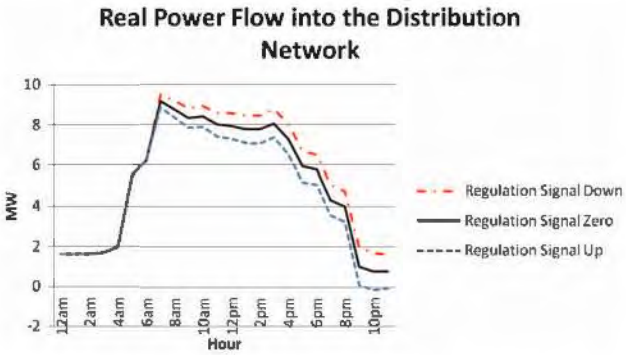

Fig. 12. *Flow of real power into the distribution network per hour.*

regulation signal were not energy neutral as we assumed here, the symmetry would not be present, and, in fact, the LMP might be different for up and down reserve provision as is the case in the ERCOT and California wholesale power markets.

Table 3 presents the payments of the inflexible loads and the income of the distributed resources in \$/MWh and \$/MVarh, respectively. It is interesting to observe the significance of reactive power's share in charges and income of inflexible load and DERs. The significance of reactive power diminishes as the supply for reactive power compensation increases, removing income opportunities from volt/var control DERs but also mitigating the cost of serving inflexible loads. The benefits to EVs from reactive power compensation and reserve provision—which, by the way, does not involve battery discharging, just flexible charging and dual use of the battery charger power electronics—is quite impressive since it renders the net cost of charging negative. As the relative size of EVs increases, however, this trend will weaken, although the benefits from offering reserves and reactive power compensation will continue to be significant.

Table 3 Charges and Income of Distribution Participants

Charges to Inflexible Loads for real power ($/MWh)	67.187
Charges to Inflexible Loads for reactive power ($/MVarh)	28.625
Charges to EV for real power ($/MWh)	90.721
Income of EV for reactive power ($/MVarh)	46.786
Income of EV for reserves ($/MWh)	48.534
Net Charges to EV per MWh consumed	-21.935
Net Income of DG for real power ($/MWh)	14.650
Income of DG for reactive power ($/MVarh)	22.693
Income of DG for reserves ($/MWh)	35.304
Total Income of DG per MWh produced	130.693
Distribution Network Rent per MWh consumed	12.909

The flow of real power into the distribution network is shown in Fig. 12.

We note that for the hours of 10 P.M. and 11 P.M. if, at some instance, all of the promised reserves happen to be deployed upward ($y = 1$), the flow of power would change directions and the distribution feeder would become a net exporter. To explore this further, we resolved the day-ahead DLMPs for a scenario where the distributed generators have a higher capacity. The resulting real power flow under a 100% reserves-up-deployment is shown in Fig. 13. In this scenario, we see a more significant reversal of flow during the 10 P.M. to 11 P.M. period. Interestingly, the DLMP of reserves and of real power falls below the reserve LMP at the substation. This is a typical result for cases of high penetration of DERs as we have seen in the 800-bus upstate NY distribution feeder; see [149]. Fig. 14 shows real power DLMP results from a high DER penetration scenario during a peak summer day in the upstate NY 800-bus distribution feeder. During high PV output hours, real power DLMPs at the PV buses close to the substation fall significantly below the LMP.

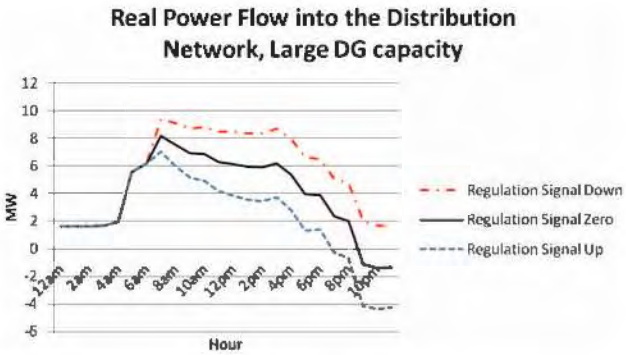

Fig. 13. *Flow of real power into the distribution network per hour for large DG capacities.*

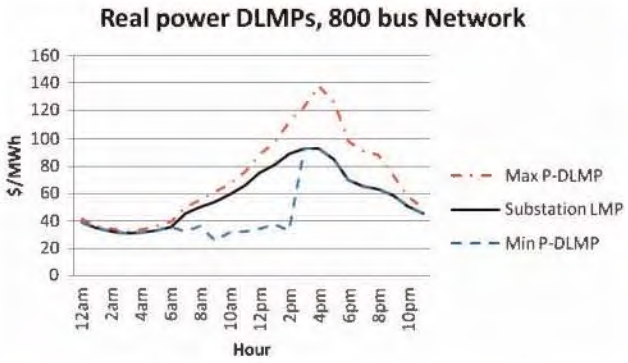

Fig. 14. *Minimum, maximum, and substation real power DLMP for an 800-bus distribution network with high distributed energy resource penetration.*

VII. CONCLUSION

We have described an extension of marginal-cost-based wholesale power markets covering today hundreds of participants to include millions of distribution-network-connected loads, generators, and distributed energy resources. Most importantly, we have characterized a tractable distributed computation and communication architecture that renders clearing of this new power market practically implementable.

Implementation of T&DLMP markets will have a profound impact on the ability and cost of securing reserves that are needed to mitigate the cost of electricity supply and enable the massive integration of renewable generation into the grid. Moreover, the successful implementation of our distributed CPS architecture framework will have a transformational impact on CPS science, engineering, and technology, as well as on CPS security.

The next steps to such a promising transformation of power markets include the following:

- the development of real size software instantiations of the proposed distributed architecture and extensive computer experimentation for proof of concept of large-scale T&DLMP market feasibility;
- the execution of field studies involving actually installed DERs, T&DLMP market clearing and DER scheduling, and monitoring of power flow through real-time sensing, and overall implementation analysis;
- extensive analysis for the identification of market malfunctions and their likelihood, followed by the study of regulatory remedies;
- development of DER subproblem optimization decision support algorithms and software;
- finally, development of communication architectures that are robust to cyberattacks and amenable to dynamic topology reconfiguration. ■

APPENDIX ON NUMERICAL RESULTS INPUT DATA

Hourly Varying Input Data

Hour	Real Power LMP ($/MWh)	Reserve LMP ($/MWh)	Demand Shape (% peak)	Solar Irradiation (% of capacity)
12am	39.04	19.52	0.1763	0
1am	34.78	17.39	0.1763	0
2am	32.34	16.17	0.1763	0
3am	30.71	15.355	0.1838	0
4am	31.46	15.73	0.2140	0.0042
5am	33.1	16.55	0.5989	0.0296
6am	35.77	17.885	0.6677	0.1534
7am	45.1	22.55	1.0000	0.3119
8am	50.08	25.04	0.9686	0.4663
9am	53.82	26.91	0.9239	0.6013
10am	59.17	29.585	0.9359	0.6923
11am	65.65	32.825	0.9032	0.7170
12pm	74.73	37.365	0.9017	0.7165
1pm	81.16	40.58	0.8896	0.6773
2pm	89.21	44.605	0.8896	0.5849
3pm	92.93	46.465	0.9221	0.4914
4pm	93.09	46.545	0.8489	0.3290
5pm	85.04	42.52	0.7168	0.1481
6pm	69.52	34.76	0.6957	0.0205
7pm	64.98	32.49	0.5485	0.0023
8pm	63.01	31.505	0.5157	0
9pm	58.66	29.33	0.2140	0
10pm	50.84	25.42	0.1838	0
11pm	45.52	22.76	0.1763	0

Transformer Data

Transformer Number	Capacity (kVA)	Hourly Cost ($)
1	10170	5.774430374
2	800	0.755308507
3	180	0.229018408
4	540	0.551527783
5	115	0.16003341
6	1205	1.048194857
7	600	0.600030584
8	700	0.678782784
9	1000	0.902926474
10	405	0.438143532
11	405	0.438143532
12	65	0.101387187
13	415	0.446777058
14	245	0.293079373
15	405	0.438143532

DER Characteristics

EV battery Capacity	24kWh
EV charging rate	3.3kW
EV charger capacity	6.6kW
DG real power generation cost	60$/MWh
DG capacity	400kW

REFERENCES

[1] M. Kranning, E. Chu, J. Lavaei, and S. Boyd, "Dynamic network energy management via proximal message passing," *Found. Trends Opt.*, vol. 1, no. 2, pp. 70–122, 2013.

[2] [Online]. Available: www.bu.edu/pcms/caramanis/ElliDistr.pdf

[3] M. C. Caramanis, E. Goldis, P. A. Ruiz, and A. Rudkevich, "Power market reform in the presence of flexible schedulable distributed loads. New bid rules, equilibrium and tractability issues," in *Proc. Allerton Conf. Commun. Control Comput.*, Oct. 1–5, 2012, pp. 1089–1096.

[4] E. Bilgin and M. C. Caramanis, "Decision support for offering load-side regulation service reserves in competitive power markets," in *Proc. IEEE Annu. Conf. Decision Control*, 2013, pp. 5628–5635.

[5] E. Ntakou and M. Caramanis, "Distribution network electricity market clearing: Parallelized PMP algorithms with minimal coordination," in *Proc. IEEE Annu. Conf. Decision Control*, 2014, pp. 1687–1694.

[6] M. Farivar and S. Low, "Branch flow model: Relaxations and convexification—Parts I & II," *IEEE Trans. Power Syst.*, vol. 28, no. 3, pp. 2554–2564, Aug. 2013.

[7] A. Q. Huang *et al.*, "Autonomous control, operation, protection of the FREEDM system," Future Renewable Electric Energy Delivery and Management Systems Center, North Carolina State Univ., Raleigh, NC, USA.

[8] Y. J.-J. Kim, L. K. Norford, and J. L. Kirtley, Jr., "Modeling and analysis of a variable speed heat pump for frequency regulation through direct load control," *IEEE Trans. Power Syst.*, vol. 30, no. 1, pp. 397–408, Jan. 2015.

[9] N. Li, L. Chen, and S. Low, "Demand response in radial distribution networks: Distributed algorithm," in *Conf. Rec. 46th Asilomar Conf. Signals Syst. Comput.*, Nov. 4–7, 2012, pp. 1549–1553.

[10] F. Schweppe, M. Caramanis, R. Tabors, and R. Bohn, *Spot Pricing of Electricity*. Norwell, MA, USA: Kluwer, 1988, pp. 355.

[11] Y. C. Paschalidis, B. Li, and M. C. Caramanis, "Demand-side management for regulation service provisioning through internal pricing," *IEEE Trans. Power Syst.*, vol. 27, no. 3, pp. 1531–1539, Aug. 2012.

[12] W. Vickrey, "Responsive pricing of public utility services," *Bell J. Econ. Manage. Sci.*, vol. 2, no. 1, 1971, pp. 337–346, DOI: 10.2307/3003171.

[13] E. Ntakou and M. Caramanis, "Distribution network spatiotemporal marginal cost of reactive power," in *Proc. IEEE Power Energy Soc. Gen. Meeting*, 2015, pp. 1–5.

[14] E. A. Goldis, M. C. Caramanis, C. R. Philbrick, A. M. Rudkevich, and P. A. Ruiz, "Security- constrained MIP formulation of topology control using loss-adjusted shift factors," in *Proc. IEEE Hawaii Int. Conf. Syst. Sci.*, 2014, pp. 2503–2509.

[15] B. Zhang, M. Caramanis, and J. Baillieul, "Control of smart building dynamic consumer preferences for efficient regulation service," in *Proc. IEEE Annu. Conf. Decision Control*, 2014, pp. 2481–2486.

[16] J. Schoene, V. Zheglov, D. Houseman, J. C. Smith, and A. Ellis, "Photovoltaics in distribution systems—Integration issues and simulation challenges," in *Proc. IEEE Power Energy Soc. Gen. Meeting*, Jul. 2013, pp. 1–5.

[17] J. M. Foster and M. C. Caramanis, "Optimal power market participation of plug-in electric vehicles pooled by distribution feeder," *IEEE Trans. Power Syst.*, vol. 28, no. 3, pp. 2065–2076, 2013.

[18] H. Chen, B. Zhang, M. C. Caramanis, and A. K. Coskun, "Data center optimal regulation service reserve provision with explicit modeling of quality of service dynamics," in *Proc. IEEE Annu. Conf. Decision Control*, 2015, pp. 7207–7213.

[19] H. Chen, A. K. Coskun, and M. C. Caramanis, "Real-time power control of data centers for providing regulation service," in *Proc. IEEE Annu. Conf. Decision Control*, 2013, pp. 4314–4321.

[20] M. J. Wainwright, T. S. Jaakkola, and A. S. Willsky, "Tree-based reparametrization framework for analysis of sum-product and related algorithms," *IEEE Trans. Inf. Theory*, vol. 49, no. 5, pp. 1120–1146, 2003.

[21] S. Boyd, K. Parikh, E. Chu, B. Peleato, and J. Eckstein, "Distributed optimization and statistical learning via the alternating direction method of multipliers," *Found. Trends Mach. Learn.*, vol. 3, pp. 1–122, 2011.

[22] E. Bilgin, M. C. Caramanis, and I. C. Paschalidis, "Smart building real time pricing for offering load-side regulation service reserves," in *Proc. IEEE Annu. Conf. Decision Control*, 2013, pp. 4341–4348.

[23] M. Caramanis, "It is time for power market reform to allow for retail customer participation and distribution network marginal pricing," *IEEE Smart Grid Newslett*, Mar. 2012.

[24] S. Chandra, D. F. Gayme, and A. Chakrabortty, "Coordinating wind farms and battery management systems for inter-area oscillation damping: A frequency-domain approach," *IEEE Trans. Power Syst.*, vol. 29, no. 3, pp. 1454–1462, 2014.

[25] M. E. Baran and F. F. Wu, "Network reconfiguration in distribution systems for loss reduction and load balancing," *IEEE Trans. Power Delivery*, vol. 4, no. 2, pp. 1401–1407, Apr. 1989.

[26] M. Kranning, E. Chu, J. Lavaei, and S. Boyd, "Dynamic network energy management via proximal message passing," *Found. Trends Opt.*, vol. 1, no. 2, pp. 70–122, 2013.

[27] M. Farivar, C. R. Clark, S. H. Low, and K. M. Chandy, "Inverter VAR control for distribution systems with renewables," in *Proc. Int. Conf. Smart Grid Commun.*, 2011, pp. 457–462.

[28] J. Lavaei, D. Tse, and B. Zhang, "Geometry of power flows in tree networks," in *Proc. IEEE Power Energy Soc. Gen. Meeting*, 2012, pp. 1–8.

[29] Q. Peng and S. H. Low, "Distributed algorithm for optimal power flow on a radial network," in *Proc. IEEE Annu. Conf. Decision Control*, 2014, pp. 167–172.

[30] M. H. Nazari and M. Ilic, "Dynamic modeling and control of distribution energy systems: Comparison with transmission power systems," *IET Gen. Transm. Distrib.*, vol. 8, no. 1, pp. 26–34, 2014.

[31] P. Ferreira, P. Carvalho, L. Ferreira, and M. Ilic, "Distributed energy resources integration challenges in low-voltage networks: Voltage control limitations and risk of cascading," *IEEE Trans. Sustain. Energy*, vol. 4, no. 1, pp. 82–88, 2013.

[32] J.-Y. Joo and M. Ilic, "Multi-layered optimization of demand resources using Lagrange dual decomposition," *IEEE Trans. Smart Grid*, vol. 4, no. 4, pp. 2081–2088, 2013.

[33] R. Verzijlbergh, M. Grond, Z. Lukszo, J. Slootweg, and M. Ilic, "Network impacts and cost savings of controlled EV charging," *IEEE Trans. Smart Grid*, vol. 3, no. 3, pp. 1203–1212, 2012.

[34] D. S. Callaway and I. A. Hiskens, "Achieving controllability of electric loads," *Proc. IEEE*, vol. 99, no. 1, pp. 184–199, Jan. 2011.

[35] Z. Ma, D. S. Callaway, and I. A. Hiskens, "Decentralized charging control of large populations of plug-in electric vehicles," *IEEE Trans. Comput. Syst. Technol.*, vol. 21, no. 1, pp. 67–78, Jan. 2013.

[36] S. Kundu and I. Hiskens, "Overvoltages due to synchronous tripping of plug-in electric-vehicle chargers following voltage dips," *IEEE Trans. Power Delivery*, vol. 29, no. 3, pp. 1147–1156, Jun. 2014.

[37] V. Kekatos, G. Wang, A.-J. Conejo, and G. B. Giannakis, "Stochastic reactive power management in microgrids with renewables," *IEEE Trans. Power Syst.*, vol. 30, no. 6, pp. 3386–3395, 2015.

[38] E. Dall'Anese, H. Zhu, and G. B. Giannakis, "Distributed optimal power flow for smart microgrids," *IEEE Trans. Smart Grid*, vol. 4, no. 3, pp. 1464–1475, 2013.

[39] N. Gatsis and G. B. Giannakis, "Decomposition algorithms for market clearing with large-scale demand response," *IEEE Trans. Smart Grid*, vol. 4, no. 4, pp. 1976–1987, 2013.

[40] S.-J. Kim and G. B. Giannakis, "Scalable and robust demand response with mixed-integer constraints," *IEEE Trans. Smart Grid*, vol. 4, no. 4, pp. 2089–2099, 2013.

[41] H. Wu, M. Shahidehpour, A. Alabdulwahab, and A. Abusorrah, "Demand response exchange in the stochastic day-ahead scheduling with variable renewable generation," *IEEE Trans. Sustain. Energy*, vol. 6, no. 2, pp. 516–525, 2015.

[42] M. Granada, M. Rider, J. Mantovani, and M. Shahidehpour, "A decentralized approach for optimal reactive power dispatch using a Lagrangian decomposition method," *Electr. Power Syst. Res.*, vol. 89, pp. 148–156, Aug. 2012.

[43] N. Lu and D. Chassin, "A state-queueing model of thermostatically controlled appliances," *IEEE Trans. Power Syst.*, vol. 19, no. 3, pp. 1666–1673, 2004.

[44] M. Galus, S. Koch, and G. Andersson, "Provision of load frequency control by PHEVs, controllable loads, a cogeneration unit," *IEEE Trans. Ind. Electron.*, vol. 58, no. 10, pp. 4568–4582, 2011.

[45] P. A. Ruiz, J. M. Foster, A. Rudkevich, and M. C. Caramanis, "Tractable transmission topology control using sensitivity analysis," *IEEE Trans. Power Syst.*, vol. 27, no. 3, pp. 1550–1559, 2012.

[46] X. Cheng and T. J. Overbye, "An energy reference bus independent LMP decomposition algorithm," *IEEE Trans. Power Syst.*, vol. 21, no. 3, pp. 1041–1049, 2006.

[47] K. W. Hedman, R. P. O'Neill, E. B. Fisher, and S. S. Oren, "Optimal transmission switching—Sensitivity analysis and extensions," *IEEE Trans. Power Syst.*, vol. 23, no. 3, pp. 1469–1479, 2008.

[48] D. P. Chassin and J. C. Fuller, "On the equilibrium dynamics of demand response," in *Proc. IEEE Hawaii Int. Conf. Syst. Sci.*, 2011, pp. 1–6.

[49] L. Chen, N. Li, S. Low, and J. Doyle, "On two market models for demand response in power networks," in *Proc. IEEE Conf. Smart Grid Commun.*, Oct. 2010, pp. 397–402.

[50] J. Lavaei and S. Low, "Zero duality gap in optimal power flow problem," *IEEE Trans. Power Syst.*, vol. 27, no. 1, pp. 92–107, 2012.

[51] A. D. Dominguez-Garcia, S. T. Cady, and C. N. Hadjicostis, "Decentralized optimal dispatch of distributed energy resources," in *Proc. IEEE Annu. Conf. Decision Control*, 2012, pp. 3688–3693.

[52] J. Warrington, P. Goulart, S. Mariethoz, and M. Morari, "A market mechanism for solving multi-period optimal power flow exactly on AC networks with mixed participants," in *Proc. IEEE Amer. Control Conf.*, 2012, pp. 3101–3107.

[53] J. Lavaei and S. Sojoudi, "Competitive equilibria in electricity markets with nonlinearities," in *Proc. IEEE Amer. Control Conf.*, 2012, pp. 3081–3088.

[54] Sathyanarayana and Heydt, "Sensitivity-based pricing and optimal storage utilization in distribution systems," *IEEE Trans. Power Delivery*, vol. 28, no. 2, pp. 1073–1082, 2013.

[55] R. A. Verzijlbergh, Z. Lukszo, J. G. Slootweg, and M. D. Ilic, "The impact of controlled electric vehicle charging on residential low voltage networks," in *Proc. Int. Conf. Netw. Sens. Control*, 2011, pp. 14–19.

[56] D. J. Hammerstrom *et al.*, "Pacific Northwest gridwise testbed demonstration projects; Part II. Grid friendly appliance project," Pacific Northwest National Laboratory (PNNL), Richland, WA, USA, Tech. Rep., 2007.

[57] FERC, "Demand response and advanced metering," Staff Rep., Oct. 2013. [Online]. Available: http://www.pjm.com/media/documents

[58] Z. Ma, D. Callaway, and I. Hiskens, "Decentralized charging control for large populations of plug-in electric vehicles," in *Proc. IEEE Annu. Conf. Decision Control*, 2010, pp. 206–212.

[59] M. Alizadeh, T.-H. Chang, and A. Scaglione, "Grid integration of distributed renewables through coordinated demand response," in *Proc. IEEE Annu. Conf. Decision Control*, 2012, pp. 3666–3671.

[60] L. Gan, U. Topcu, and S. Low, "Optimal decentralized protocol for electric vehicle charging," in *Proc. IEEE Annu. Conf. Decision Control/Eur. Control Conf.*, 2011, pp. 5798–5804.

[61] W. Zhang, K. Kalsi, J. Fuller, M. Elizondo, and D. Chassin, "Aggregate model for heterogeneous thermostatically controlled loads with demand response," in *Proc. IEEE Power Energy Soc. Gen. Meeting*, 2012, pp. 1–8.

[62] M. D. Ilic, L. Xie, and J.-Y. Joo, "Efficient coordination of wind power and price-responsive demand—Part I: Theoretical foundations," *IEEE Trans. Power Syst.*, vol. 26, no. 4, pp. 1875–1884, 2011.

[63] S. Meyn, P. Barooah, A. Busic, and J. Ehren, "Ancillary service to the grid from deferrable loads: The case for intelligent pool pumps in Florida," in *Proc. IEEE Annu. Conf. Decision Control*, 2013, pp. 6946–6953.

[64] E. Litvinov, T. Zheng, G. Rosenwald, and P. Shamsollahi, "Marginal loss modeling in LMP calculation," *IEEE Trans. Power Syst.*, vol. 19, no. 2, pp. 880–888, 2004.

[65] H. Wang, J. Huang, X. Lin, and H. Mohsenian-Rad, "Exploring smart grid and data center interactions for electric power load balancing," *ACM SIGMETRICS*, vol. 41, no. 3, pp. 89–94, 2013.

[66] X. Zhan and S. Reda, "Techniques for energy-efficient power budgeting in data centers," in *Proc. 50th Annu. Design Autom. Conf.*, 2013.

[67] B. Lesieutre, S. Roy, V. Donde, and A. Pinar, "Power system extreme event screening using graph partitioning," Lawrence Berkeley Nat. Lab., LBNL-61600, 2006.

[68] I. Dobson, M. Parashar, and C. Carter, "Combining phasor measurements to monitor cutset angles," in *Proc. IEEE Hawaii Int. Conf. Syst. Sci.*, 2010, pp. 1–9.

[69] J. L. Willems and J. C. Willems, "The application of lyapunov methods to the computation of transient stability regions for multimachine power systems," *IEEE Trans. Power Apparatus Syst.*, vol. PAS-89, no. 5/6, pp. 795–801, 1970.

[70] A. Chakrabortty and C. F. Martin, "Spatial allocation of phasor measurements for parametric model identification of power systems," *IEEE Trans. Comput. Syst. Technol.*, vol. 22, no. 5, pp. 1801–1812, 2014.

[71] A. Chakrabortty, "Wide-area damping control of power systems using dynamic clustering and TCSC-based redesigns," *IEEE Trans. Smart Grid*, vol. 3, no. 3, pp. 2493–2498, Sep. 2012.

[72] A. Chakrabortty, J. H. Chow, and A. Salazar, "A measurement-based framework for dynamic equivalencing of power systems using wide-area phasor measurements," *IEEE Trans. Smart Grid*, vol. 1, no. 2, pp. 68–81, 2011.

[73] S. Nabavi and A. Chakrabortty, "Graph-theoretic conditions for global identifiability of weighted consensus networks," *IEEE Trans. Autom. Control*, vol. 61, no. 2, pp. 497–502, 2016.

[74] D. Soudbaksh, A. Chakrabortty, and A. Annaswamy, "Delay-aware co-designs for wide-area control of power grids," in *Proc. IEEE Annu. Conf. Decision Control*, 2014, pp. 2493–2498.

[75] K. Marzullo, "Tolerating failures of continuous-valued sensors," *ACM Trans. Comput. Syst.*, vol. 8, no. 4, pp. 284–304, Nov. 1990.

[76] C. De Persis and P. Tesi, "Resilient control under denial-of-service." [Online]. Available: http://arxiv.org/abs/1311.5143

[77] J. Zhang, P. Jaipuria, A. Hussain, and A. Chakrabortty, "Attack-resilient estimation of power system oscillation modes using distributed and parallel optimization: Theoretical and experimental methods," in *Proc. Conf. Decision Game Theory Security*, Los Angeles, CA, 2014, pp. 350–359.

[78] D. F. Gayme and A. Chakrabortty, "Using wind farm siting and control for shaping inter-area oscillations in large power systems," *IEEE Trans. Comput. Syst. Technol.*, vol. 22, no. 4, 2014.

[79] S. Chandra, D. Mehta, and A. Chakrabortty, "Exploring impact of wind penetration on power system equilibrium using a numerical continuation approach," in *Proc. IEEE Amer. Control Conf.*, 2015, pp. 4339–4344.

[80] J. Baillieul, B. Zhang, and S. Wang, "The Kirchhoff-Braess paradox and its implications for smart microgrids," in *Proc. IEEE CCD*, 2015, pp. 6556–6573.

[81] B. Zhang and J. Baillieul, "A packetized direct load control mechanism for demand side management," in *Proc. IEEE Annu. Conf. Decision Control*, 2012, pp. 3658–3665.

[82] B. Zhang and J. Baillieul, "A novel packet switching framework 'with binary information in demand side management," in *Proc. IEEE Annu. Conf. Decision Control*, 2013, pp. 4957–4963.

[83] B. Zhang and J. Baillieul, "A two level feedback system to provide regulation reserve," in *Proc. IEEE Annu. Conf. Decision Control*, 2013, pp. 4322–4328.

[84] B. Zhang and J. Baillieul, "Communication and control protocols for load networks in the smart grid," in *Proc. IFAC*, Cape Town, South Africa, Aug. 25–29, 2014, pp. 11 250–11 256.

[85] B. Zhang, M. C. Caramanis, and J. Baillieul, "Optimal price-controlled demand response with explicit modeling of consumer preference dynamics," in *Proc. IEEE Annu. Conf. Decision Control*, 2014, pp. 2481–2486.

[86] B. Zhang and J. Baillieul, "Control and communication protocols that enable smart building microgrids," *Proc. IEEE*, vol. 104, no. 4, Apr. 2016, DOI: 10.1109/JPROC.2016.2520759.

[87] R. E. Brown, "Impact of smart grid on distribution system design," in *Proc. IEEE Power Energy Soc. Gen. Meeting—Conversion and Delivery of Electrical Energy in the 21st Century*, 2008, pp. 1–4.

[88] S. Massoud Amin and B. F. Wollenberg, "Toward a smart grid: Power delivery for the 21st century," *IEEE Power Energy Mag.*, vol. 3, no. 5, pp. 34–41, Sep./Oct. 2005, DOI: 10.1109/MPAE.2005.1507024.

[89] G. Celli *et al.*, "Meshed vs. radial MV distribution network in presence of large amount of DG," in *Proc. IEEE PES Power Syst. Conf. Expo.*, 2004, vol. 2, pp. 709–714.

[90] S. Wang, J. Baillieul, and B. Zhang, "The inevitable loss effect of electrical network capacity enhancement," Intell. Mechatron. Lab, Boston Univ., Boston, MA, USA, preprint, 2015.

[91] General Electric, "Digital energy—Modernizing the grid," 2015. [Online]. Available: https://www.gedigitalenergy.com/multilin/resource/Feeder/UniFlip_Publication/document.pdf

[92] Q.-C. Zhong and T. Hornik, *Control of Power Inverters in Renewable Energy and Smart Grid Integration*. West Sussex, U.K.: Wiley/IEEE Press, 2013, ISBN: 13: 978-0470667095, ISBN: 10: 0470667095.

[93] A. K. Coskun, "HotSpot 3D extension", Boston Univ., Boston, MA, USA. [Online]. Available: http://www.bu.edu/peaclab/research/tools-and-software/

[94] T. Zhang *et al.*, "3D-MMC: A modular 3D multi-core architecture with efficient

resource pooling," in *Proc. Design Autom. Test Eur. Conf. Exhibit.*, 2013, pp. 1241–1246.

[95] J. Meng, K. Kawakami, and A. K. Coskun, "Optimizing energy efficiency of 3-D multicore systems with stacked dram under power and thermal constraints," in *Proc. 49th Annu. Design Autom. Conf.*, 2012, pp. 648–655.

[96] J. Meng, T. Zhang, and A. Coskun, "Dynamic cache pooling for improving energy efficiency in 3D stacked multicore processors," in *Proc. IFIP/IEEE Int. Conf. Very Large Scale Integr.*, 2013, pp. 210–215.

[97] M. M. Sabry, A. Sridhar, J. Meng, A. K. Coskun, and D. Atienza, "Greencool: An energy-efficient liquid cooling design technique for 3- D MPSOCs via channel width modulation," *IEEE Trans. Comput.-Aided Design Integr. Circuits Syst.*, vol. 32, no. 4, pp. 524–537, 2013.

[98] T. Zhang, J. Meng, and A. K. Coskun, "Dynamic cache pooling in 3D multicore processors," *ACM J. Emerging Technol. Comput. Syst.*, vol. 1, no. 1, Article 1, pp. 210–215, 2015.

[99] T. Zhang, J. Abellan, A. Joshi, and A. Coskun, "Thermal management of manycore systems with silicon-photonic networks," in *Proc. Design Autom. Test Eur. Conf. Exhibit.*, Mar. 2014, pp. 1–6.

[100] D. Chen, A. Q. Huang, Y. Xu, F. Wang, and W. Yu, "Distributed and autonomous control of the FREEDM system a power electronics based distribution system," in *Proc. IECON*, Oct. 2014, pp. 4954–4960.

[101] N. T. Gayeski, P. R. Armstrong, and L. K. Norford, "Predictive cooling of thermo-active building systems with low-lift chillers," *HVAC&R Res.*, vol. 18, no. 5, pp. 858–873, 2012.

[102] T. Zakula, N. T. Gayeski, P. R. Armstrong, and L. K. Norford, "Variable-speed heat pump model for a wide range of cooling conditions and loads," *HVAC&R Res.*, vol. 17, no. 5, pp. 670–691, 2011.

[103] T. Zakula, P. R. Armstrong, and L. K. Norford, "Optimal coordination of heat pump compressor and fan speed and subcooling over a wide range of loads and conditions," *HVAC&R Res.*, vol. 18, no. 6, pp. 1153–1167, 2012.

[104] T. Zakula, L. Norford, and P. Armstrong, "Modeling environment for model predictive control of buildings," *Energy Buildings*, vol. 85, pp. 549–559, 2014.

[105] T. Zakula, L. Norford, and P. Armstrong, "Advanced cooling technology with thermally activated building surfaces and model predictive control," *Energy Buildings*, vol. 86, pp. 640–650, 2015.

[106] D. H. Blum, T. Zakula, and L. K. Norford, "Variable cost quantification for ancillary services provided by heating, ventilating and air-conditioning systems," *IEEE Trans. Smart Grid*, 2016.

[107] L. Su and L. K. Norford, "Demonstration of HVAC chiller control for power grid frequency regulation—Part 1: Controller development and experimental results," *HVAC&R Res.*, vol. 21, no. 8, 2015, pp. 1134–1142.

[108] L. Su and L. K. Norford, "Demonstration of HVAC chiller control for power grid frequency regulation—Part 2: Discussion of results and considerations for broader deployment," *HVAC&R Res.*, vol. 21, no. 8, 2015 pp. 1143–1153.

[109] M. R. Jongerden and B. R. Haverkort, "Which battery model to use?" *IET Softw.*, vol. 3, no. 6, pp. 445–457, 2009.

[110] B. Schweighofer *et al.*, "Fast and accurate battery model applicable for EV and HEV simulation," in *Proc. IEEE Int. Instrum. Meas. Technol. Conf.*, 2012, pp. 565–570.

[111] E. M. Ryan *et al.*, "Computational modeling of transport limitations in li-air batteries," *Meeting Abstracts*, no. 6, pp. 155–155, 2012.

[112] E. M. Ryan *et al.*, "A damage model for degradation in the electrodes of solid oxide fuel cells: Modeling the effects of sulfur and antimony in the anode:," *J. Power Sources*, vol. 210, pp. 233–242, 2012.

[113] J. Tan and E. M. Ryan, "Dendrite growth in a li-air battery," in *Proc. 223rd Electrochem. Soc. Meeting*, 2013.

[114] J. Tan, A. Tartakovsky, and E. M. Ryan, "Suppressing dendritic growth in lithium batteries through anisotropic transport," *J. Electrochem. Soc.*, vol. 163, no. 2, 2016, pp. A318–A327.

[115] W. A. Lane *et al.*, "Numerical modeling and uncertainty quantification of a bubbling fluidized bed with immersed horizontal tubes," *Powder Technol.*, vol. 253, no. 0, pp. 733–743, 2014.

[116] C. B. Storlie *et al.*, "Calibration of computational models with categorical parameters and correlated outputs via Bayesian smoothing spline," *ANOVA J. Amer. Stat. Assoc.*, vol. 110, no. 509, pp. 68–82, 2015.

[117] W. W. Hogan, "Back cast of interim solution B + to improve real-time scarcity pricing," ERCOT, white paper, 2013. [Online]. Available: http://www.ercot.com/content/news/presentations/2013/White Paper—Back Cast of Interim Solution B+ to Improve Re.pdf

[118] P. R. Gribik, W. W. Hogan, and S. L. Pope, "Market-clearing electricity prices and energy uplift," 2007. [Online]. Available: http://www.hks.harvard.edu/fs/whogan/Gribik_Hogan_Pope_Price_Uplift_123107.pdf

[119] W. W. Hogan, "Electricity scarcity pricing through operating reserves," *Econom. Energy Environ. Policy*, vol. 2, no. 2, pp. 65–86, 2013.

[120] Monitoring Analytics, "2013 state of the market report for PJM—Volume 2," 2014. [Online]. Available: http://www.monitoringanalytics.com/reports/pjm_state_of_the_market/2013/2013-som-pjm-volume2.pdf

[121] G. Wang, U. V. Shanbhag, T. Zheng, E. Litvinov, and S. Meyn, "An Extreme-point subgradient method for convex hull pricing in energy and reserve markets—Part I: Algorithm structure," *IEEE Trans. Power Systems*, vol. 28, no. 3, pp. 2111–2120, Aug. 2013.

[122] J. Wang, P. M. S. Carvalho, and J. Kirtley, "Emergency reconfiguration and distribution system planning under the Single-Contingency Policy," in *Proc. IEEE PES Innovative Smart Grid Technol.*, Jan. 2012, pp. 1–5.

[123] A. Moawwad, V. Khadkikar, and J. L. Kirtley, "Interline photovoltaic (I-PV) power plants for voltage unbalance compensation," in *Proc. IEEE IES Conf.*, 2012, pp. 5330–5334.

[124] Li and Na, "A market mechanism for electric distribution networks," in *Proc. IEEE Annu. Conf. Decision Control*, 2015, pp. 2276–2272.

[125] E. Ntakou and M. Caramanis, "Enhanced convergence rate of inequality constraint shadow prices in PMP algorithm cleared distribution power markets," in *Proc. Amer. Control Conf.*, 2016, to be published.

[126] F. C. Schweppe, "Power systems 2000: Hierarchical control strategies," *IEEE Spectrum*, vol. 15, no. 7, pp. 42–47, Jul. 1978.

[127] N. Miller, M. Shao, S. Pajic, and R. D'Aquila, "Eastern frequency response study," GE Energy, Tech Rep. NREL/SR-5500-58077, May 2013.

[128] R. Wiser and M. Bolinger, "Wind technologies market report," 2011. [Online]. Available: www1.eere.energy.gov/wind/pdfs/2011_wind_technologies_market_report.pdf

[129] M. J. Krok and S. Genc, "A coordinated optimization approach to volt/var control for large power distribution networks," in *Proc. Amer. Control Conf.*, Jun. 2011, pp. 1145–1150.

[130] E. Ela, M. Milligan, and B. Kirby, "Optimal reserves and variable generation," Nat. Renewable Energy Labs, Tech. Rep. NREL/TP-5500-51978, Aug. 2011.

[131] U.S. Energy Information Administration (EIA), "Average operating heat rate for selected energy sources." [Online]. Available: www.eia.gov/electricity/anual/html/epa_08_01.html

[132] U.S. Energy Information Administration (EIA), "How much electricity is lost in transmission and distribution in the US?" [Online]. Available: www.eia.gov/tools/faqs/faq.cfm?id=105&t-3

[133] M. Milligan *et al.*, "Operating reserves and wind power integration: An international comparison," NREL/CP-5500-49019, Oct. 2010.

[134] N. W. Miller, M. Shao, and S. Venkataraman, "California ISO (CAISO) frequency response study," GE Energy, Tech. Rep., Nov. 2011.

[135] ERCOT, "Future ancillary services in ERCOT," concept paper, 2013, ver. 1.0.

[136] M. Drouineau, N. Maizi, and V. Mazauric, "Impacts of intermittent sources on the quality of power supply: The key role of reliability indicators," *App. Energy*, vol. 116, pp. 333–343, 2014.

[137] NYS Department of Public Service Staff Report and Proposal, "Reforming the energy vision," Case 14-M-0101, 2014.

[138] ARPA-E U.S. Dept. Energy, "Network optimized distributed energy systems (NODES)," FOA no. DE-FOA-0001289, CFDA no. 81.135, Modification 02, Jun. 2015. [Online]. Available: https://arpa-e-foa.energy.gov/#Foaldc039dfd3-ae21-47e7-801c-fd13b2bf18ad

[139] P. A. Ruiz *et al.*, "Reduced MIP formulation for transmission topology control," in *Proc. Allerton Conf.*, Oct. 1–5, 2012, pp. 1073–1079.

[140] E. Goldis *et al.*, "Applicability of topology control algorithms (TCA) to a real-size power system," in *Proc. Allerton Conf.*, 2013, pp. 1349–1352.

[141] E. A. Goldis, X. Li, M. C. Caramanis, A. M. Rudkevich, and P. A. Ruiz, "AC-based topology control algorithms (TCA)—A PJM historical data case study," in *Proc. IEEE Hawaii Int. Conf. Syst. Sci.*, 2015, pp. 2616–2619.

[142] A. Ott, "Experience with PJM market: Operation, system design, implementation,"

IEEE Trans. Power Syst., vol. 18, no. 2, pp. 528–534, 2003.

[143] A. Ott, "Evolution of computing requirements in the PJM market: Past and future," in *Proc. IEEE Power Energy Soc. Gen. Meetings*, Jul. 25–29, 2010, pp. 1–4.

[144] U.S. Dept. Energy, "Strategic plan, 2014-2018." [Online]. Available: http://energy.gov/sites/prod/files/2014/04/f14/2014_dept_energy_strategic_plan.pdf

[145] K. Mamandur and R. Chenoweth, "Optimal control of reactive power flow for improvements in voltage profiles and for real power loss minimization," *IEEE Trans. Power Apparatus Syst.*, vol. 100, no. 7, pp. 3185–3194, 1981.

[146] Y. Makarov, C. Loutan, J. Ma, and P. de Mello, "Operational impacts of wind generation on California power systems," *IEEE Trans. Power Syst.*, vol. 24, no. 2, pp. 1039–1050, May 2009.

[147] M. C. Caramanis and J. M. Foster, "Coupling of day ahead and real time power markets for energy and reserves incorporating local distribution network costs and congestion," in *Proc. Allerton Conf.*, 2010, pp. 42–49.

[148] E. Bilgin, M. Caramanis, I. Paschalidis, and C. Cassandras, "Provision of regulation service by smart buildings," *IEEE Trans. Smart Grid*, 2015, to be published.

[149] New York State Energy Research and Development Authority (NYSERDA), "Developing competitive electricity markets and pricing structures," white paper, 2016.

[150] J. Ponniah, Y. Hu, and P. R. Kumar, "A clean slate approach to secure wireless networking," *Found. Trends Netw.*, vol. 9, no. 1, pp. 1–105, 2015.

[151] M. Liao and A. Chakrabortty, "A round-robin ADMM algorithm for identifying data-manipulators in power system estimation," in *Proc. Amer. Control Conf.*, 2016, to be published.

[152] D. Kempe, A. Dobra, and J. Gehrke, "Gossip-based computation of aggregate information," in *Proc. 44th Annu. IEEE Symp. Found. Comput. Sci.*, 2003, pp. 482–491.

[153] D. Shah and M. Crow, "Stability design criteria for distribution systems with solid-state transformers," *IEEE Trans. Power Delivery*, vol. 29, no. 6, pp. 2588–2595, 2014.

ABOUT THE AUTHORS

Michael Caramanis (Senior Member, IEEE) received the B.S. degree in chemical engineering from Stanford University, Stanford, CA, USA, in 1971 and the M.S. and Ph.D. degrees in engineering from Harvard University, Cambridge, MA, USA in 1972 and 1976, respectively.

He has been a Professor of Systems and Mechanical Engineering at Boston University, Boson, MA, USA, since 1982. He chaired the Greek Regulatory Authority for Energy and the International Energy Charter's Investment Group (2014–2008), was personally involved in power market implementations in England (1989–1990) and Italy (2000–2003), and his written work has influenced Power Market design in the United States and Europe. His current application domain focus is marginal costing and dynamic pricing on smart power grids, grid topology control for congestion mitigation, and the extension of power markets to include distribution connected loads, generation, and resources. He is coauthor of *Spot Pricing of Electricity* (Norwell, MA, USA: Kluwer, 1987) and more than 100 refereed publications. His disciplinary background is in mathematical economics, optimization, and stochastic dynamic decision making.

William W. Hogan received the B.S. degree in engineering from the U.S. Air Force Academy, CO, USA, in 1966 and the MBA degree in business administration and Ph.D. degree in operations research from the University of Los Angeles (UCLA), Los Angeles, CA, USA , in 1967 and 1971, respectively.

He is the Raymond Plank Professor of Global Energy Policy at the JFK School of Government, Harvard University, Cambridge, MA, USA. He is Research Director of the Harvard Electricity Policy Group in the Mossavar-Rahmani Center for Business and Government and a longtime member of the Kennedy School Faculty Appointments Committee. He served on the faculty of Stanford University, Stanford, CA, USA, where he founded the Energy Modeling Forum (EMF). His research focuses on the interaction of energy economics and public policy, with an emphasis on the restructuring of the electricity industry in the United States and worldwide. He has worked to design the market structures and market rules by which regional transmission organizations coordinate bid-based markets for energy, ancillary services, and financial transmission rights. Selected papers are available on his website, www.whogan.com.

Prof. Hogan is Past President of the International Association for Energy Economics (IAEE).

Elli Ntakou (Student Member, IEEE) received the B.S. degree in electrical and computer engineering (*summa cum laude*), with a major in energy systems and a minor in electronics, from the National Technical University of Athens, Athens, Greece, in 2011 and the M.S. degree in systems engineering with a concentration in operations research from Boston University, Boston, MA, USA, in 2014, where she is currently working toward the Ph.D. degree in the division of Systems Engineering, working in the area of distribution network electricity markets.

Her research interests include power systems, smart grid, market economics and design, optimization, and big data.

Aranya Chakrabortty (Senior Member, IEEE) received the B.E. degree in electrical engineering from Jadavpur University, Kolkata, India, in 2004 and the M.S. and Ph.D. degrees in electrical engineering from Rensselaer Polytechnic Institute, Troy, NY, USA, in 2005 and 2008, respectively.

He was a Postdoctoral Research Associate at the University of Washington, Seattle, WA, USA, in 2009. Since 2010, he has been an Associate Professor of Electrical and Computer Engineering at North Carolina State University, Raleigh, NC, USA. His research interests are in all branches of control theory, and their applications to power system dynamics and control using emerging technologies such as wide-area measurement systems (WAMSs). He is coeditor of the book *Control and Optimization Methods for Electric Smart Grids* (New York, NY, USA: Springer-Verlag, 2012) and more than 70 refereed conference and journal publications.

Dr. Chakrabortty contributes actively to the North American Synchrophasor Initiative (NASPI). He received the National Science Foundation (NSF) CAREER award in 2011.

Jens Schoene (Member, IEEE) received the Diplom-Ingenieur degree from the University of Paderborn, Dept. Soest, Germany, and the M.S. and Ph.D. degrees from the University of Florida, Gainesville, FL.

He is the Director of Research Studies at EnerNex, Knoxville, TN. His areas of expertise are the transient and harmonic analysis of power systems, distributed generation interconnection studies, induction studies, lightning studies, and arc flash studies. His research at the International Center for Lightning Research and Testing (ICLRT) at the University of Florida, Gainesville, FL, USA, involved the interaction of lightning with power distribution lines, grounding systems of residential houses and explosive storage bunkers, and aircrafts. He published eight scientific papers as main author and ten scientific papers as coauthor in peer-reviewed journals. He is the main author or coauthor of over 25 conference proceedings.

Dr. Schoene is actively involved in the IEEE Power and Energy Society (PES) "Wind Plant Collector System Design" Working Group and the "Stray and Contact Voltage" Working Group. He is the Vice Chair of the IEEE PES "Lightning Performance of Overhead Lines" Working Group.